

The study of the Taftan- Bazman volcanic area, South-eastern Iran and its relation with Makran-Chagai Volcanic Arc.

A Thesis

Submitted to

Indian Institute of Science Education and Research, Pune in partial fulfilment of the requirements for the BS-MS Dual Degree Programme

By

Shubhangi Khobragade

(20151009)



Indian Institute of Science Education and Research, Pune
Dr. Homi Bhabha Road,
Pashan, Pune 411008, INDIA.

April, 2020

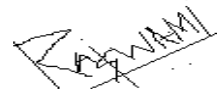
Supervisor: Dr. Raymond Duraiswami, SPPU, Pune

Shubhangi Khobragade

All rights reserved

Certificate

This is to certify that this dissertation entitled “**The study of the Taftan-Bazman volcanic area, South-eastern Iran and its relation with Makran-Chagai volcanic arc.**”, towards the partial fulfilment of the BS-MS dual degree programme at the Indian Institute of Science Education and Research, Pune, represents study/work carried out by Shubhangi Khobragade at Savitribai Phule Pune University, Pune and IISER Pune, under the supervision of Dr. Raymond Duraiswami, Professor of Geology, Department of Geology, SPPU, Pune, during the academic year 2019-2020.



Dr. Raymond Duraiswami
SPPU, Pune

Committee: Earth and Climate
Sciences

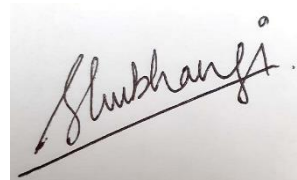
Dr. Raymond Duraiswami

Prof. Shyam S. Rai

Date: 28th March 2019

Declaration

I hereby declare that the research work presented in the report entitled “**The study of the Taftan- Bazman volcanic area, South-eastern Iran and its relation with Makran-Chagai volcanic arc.**” have been carried out by me at Department of Geology, SPPU & IISER Pune under the supervision of Dr. Raymond A. Duraiswami and the same has not been submitted elsewhere for any other degree.

A photograph of a handwritten signature in black ink on a white background. The signature is written in a cursive style and reads "Shubhangi".

Shubhangi Khobragade

Date: 28th March 2019

Acknowledgements

This thesis wouldn't have been possible without the efforts and motivation of many people. I am very grateful to my supervisor Dr Raymond A. Duraiswami, who firstly accepted me for the MS-Thesis project. I will forever be grateful to him for giving me this opportunity. He has always motivated and guided me throughout the project. I have learned a lot under his guidance. This knowledge gained will be beneficial to me for my future career. His cheerful and helpful nature has always inspired me and truly helped in my growth as a student. I am honoured to have him as my mentor.

I would also like to express my gratitude to Prof Shyam S Rai for all the help and constant guidance whenever needed. His experience and knowledge were very helpful for my project. He has also been a source of true motivation to me and gave important insights and instructions which proved beneficial to me. He has always been very kind and upfront for all the support.

I also thank Prof N. R. Karmalkar from Pune University for allowing me to use the necessary labs and instruments to carry out the experiments at the Department of Geology.

I am thankful to the PhD students from IISER Pune and Pune University, especially Mr Gokul Saha and Mohammad Noor respectively. Their help means a lot to me. I am thankful to Sourajit Sahoo my junior BS-MS 3rd Yr for all the help during my project. His suggestions and scooter ride to Pune University helped me at the difficult times.

My friends Bhawana, Devesh, Nikhil, Jaideep, Jyotish, Shubham, Tushar have motivated and helped me throughout this project.

I would also like to thank my family for constant support. I will always be grateful to them for all their efforts.

Contents

List of Figures	7
List of tables	8
ABSTRACT.....	9
1. INTRODUCTION	10
1.1 Study Area.....	10
1.2 Scope of Thesis.....	10
1.3 Volcanic Rocks.....	11
1.4 Objectives.....	12
2. MATERIALS AND METHODS	14
2.1 Literature Work	14
2.2 Field Visit and Rock Sampling.....	14
2.3 Sample preparation for Petrography and geochemical analysis.....	14
2.3.1 Thin-section Preparation.....	16
2.3.2 Powdering rock samples for geochemical analysis.....	12
2.4 Petrographic Study.....	17
2.5 Plotting Earthquake Distribution for the study area	17
2.6 Geochemical analysis	18
2.6.1 Acid Dissolution.....	18
2.6.2 XRF sample loading.....	18
2.7 Making cross-section maps using Earthquake data.....	19
3. RESULTS.....	19
3.1 Thin-section Observations.....	19
3.1.1 Textural Study and Petrography.....	19

3.1.1.1 Petrography of Quenched Pyroxene.....	19
3.1.1.2 Petrography of sieved Pyrx and zoned Plag.....	20
3.1.1.3 Petrography of Prismatic Pyrx and zoned Plag.....	21
3.1.1.4 Petrography of shattered Pyrx and zoned Plag.....	22
3.1.1.5 Petrography of reabsorbed Pyrx and strained vesicles.....	23
3.1.1.6 Petrography of altered Pyrx.....	24
3.1.1.7 Petrography of deformed vesicles.....	25
3.1.1.8 Petrography of altered skeletal Pyrx.....	26
3.2 Results of Geochemical analysis.....	27
3.2.1 Major oxide analysis.....	27
3.2.2 Trace element analysis.....	30
3.3 Earthquake Distribution of the study area.....	34
3.4 Cross-section profiles of the study area.....	34
3.4.1 Transect along 60E, 25N – 62E, 35N.....	35
3.4.2 Transect along 63E, 25N – 65E, 35N.....	36
3.4.3 Transect along 64E, 25N – 61E, 35N.....	37
3.4.4 Transect along 60E, 28N – 67E, 30N.....	39
4. DISCUSSIONS.....	40
4.1 Petrography.....	40
4.2 Geochemistry.....	40
4.3 Cross-sectional Profiles (seismic velocity vs depth).....	41
5. CONCLUSIONS.....	42
6. REFERENCES.....	42

List of Figures

Figure 1	Geological map of Iran showing major volcanoes (modified after Geological Survey & Mineral Exploration of Iran, 2005; (Richard et al., 2006).	6
Figure 2	Google Earth image of the Bazman and Taftan volcanic fields, Sistan and Baluchestan province, Iran.	8
Figure 3	Field photograph of Taftan stratovolcano.	10
Figure 4	Field photograph of Bazman stratovolcano	12
Figure 5	The procedure of powdering rocks using hand agate motor	13
Figure 6	The above image shows a thin-section slide and the petrological microscope	16
Figure 7	The above image shows the filtering of dissolved rock samples for ICPMS analysis	16
Figure 8	Photomicrograph showing quenched Pyroxene crystal	18
Figure 9	Photomicrograph showing zoned Plagioclase and reabsorbed Pyroxene crystal	19
Figure 10	Photomicrograph showing prismatic Pyroxene and zoned Plagioclase crystal	21
Figure 11	Photomicrograph showing shattered Pyroxene and zoned Plagioclase crystal	22
Figure 12	Photomicrograph showing strained vesicles and reabsorbed pyroxene crystal	23
Figure 13	Photomicrograph slide showing altered Pyroxene and mesostatis glass needles in the ground mass	24
Figure 14	Photomicrograph showing deformed spherical vesicles	27
Figure 15	Photomicrograph showing skeletal Pyroxene	28
Figure 16	Geochemical plots. (a) AFM diagram (b) PI vs. ASI (c) $\text{Na}_2\text{O}+\text{K}_2\text{O}$ vs SiO_2	29
Figure 17	Geochemical plots. (a) Total alkali–silica (TAS) diagram (b) Nb/Zr vs. SiO_2 (c) SiO_2 vs Zr / TiO_2	32
Figure 18	Earthquake distribution with variation in magnitude and depth of earthquakes over the Iran region	34
Figure 19	Cross-section profile along 60E, 25N – 62E, 35N on the Iran map	35
Figure 20	Cross-section profile along 63E, 25N – 65E, 35N on the Iran map	36
Figure 21	Cross-section profile along 64E, 25N – 61E, 35N on the Iran map	38
Figure 22	Cross-section profile along 60E, 28N – 67E, 30N on the Iran map	39

List of tables

Table 1	Major oxide (wt. %) of rocks from the Taftan and Bazman volcanoes	27
Table 2	Trace elements (ppm) of rocks from the Taftan and Bazman volcanoes	31

ABSTRACT

The Makran-Chagai volcanic arc transcends the Pakistan-Iran border and contains numerous strato-volcanoes prominent being the Kuh-e-Sultan, Kuh-e-Taftan, Kuh-i-Bazman and the Shahsavaran volcanic fields. Volcanism in this region dates from 6.95 Ma to 0.71 Ma. Our study relates to the Taftan-Bazman volcanic region of Sistan and Baluchestan province, Iran.

We undertook a two pronged approach during this dissertation. One was to use field mapping and petrogeochemistry to evaluate the nature of the volcanism, their products and understand their petrogenesis. The second was to collect and collate seismic data and model the same to prepare cross sections along and across the magmatic arc so as to decipher the structure of below and comment on the status (dormant/extinct) of the arc volcanism.

The stratovolcanoes of Taftan and Bazman have widespread pyroclastic ash, pumice and ignimbrites with fewer but thicker lava flows. Based on already published geochemical datasets and our own analyses suggest that the volcanism is represented by a calc-alkaline basaltic andesite-dacite-rhyolite volcanism for the Taftan-Bazman stratovolcanoes. Based on this it is clear that the Taftan-Bazman volcanic fields are related to the older (2.5 Ma to present) Makran-Chagai volcanic arc related to the subduction of the Oman plate below the Lut-Afghan block.

Modelling of real time seismic data from IRIS and EHB produced several cross section profiles along and cross the Makran-Chagai volcanic arc. A band of high velocity zone extends from the edge of the Oman Sea and beyond the Taftan volcano at depths of 70 to 100 km bgl. The traverse along the Makran-Chagai volcanic arc show similar patterns of the high velocity zone, but the zone diminishes towards the west and a feeble signature is seen below Bazman. Evidence of present day fumarolic activity and the shallowing of the high velocity zone below Taftan suggest that volcano is rather dormant than extinct. Dormancy of stratovolcanoes in Island arc settings can exist from 100 to 300 years and any eruption in the near future could at least be of Vulcanian to sub-pilinian type.

1. INTRODUCTION

1.1 Study area

This study deals with the geographical area of the south-eastern part of Iran (Fig. 1.1), namely Makran. Makran region is the result of Arabian and Eurasian plate collision. The Arabic Plate subducts beneath the Eurasian Plate, and resultant is the subduction zone along the Gulf of Oman margin. This Makran trench is vicinal to the Baluchestan area of Pakistan. The Shallow subduction along this margin generated the Makran-Chagai arc, which generated the volcanoes like Bazman, Taftan and Kuh-i-Sultan. This study covers Bazman and Taftan and also the adjacent Bazo volcanic fields.

The Bazman volcano (3490 m amsl) is the part of the Makran-Chagai volcanic arc located in South-eastern Iran. It comes under the Sistan and Baluchestan Province. As seen from the satellite, there exists a conical summit of Bazman volcano. The crater is approximately 500 meters wide. The Bazman volcano consists mainly of andesite and dacite volcanic rocks. There are no past recorded eruptions but the Bazman volcano, but it does have fumaroles, therefore, can be considered to be dormant but not extinct (<https://en.wikipedia.org>). The Moho beneath Bazman is approximately at a depth of 48-50 km (Abdetedal et al., 2014). This volcano is considered to be of Quaternary age. As reported by Conrad et al. (1981), the K-Ar ages of 3 Bazman lava flows recorded are 11.5, 4.7 and 0.7 Ma respectively.

The Taftan Volcano (4000 m amsl) lies in the middle of the East-West trending Makran-Chagai Magmatic arc. It is located near the city of Khas. The stratovolcano Kuh-e-Taftan is locally known as “blistering, smoldering, fuming mountain of Taftan”. This volcano is considered to be semi-active and young because there are reports of molten sulphur flow in 1993. At the summit of the volcano, active fumaroles with high concentrations of sulphur are found. According to Siebert and Sikkim (2002), in 1902, the Taftan volcano reported to be smoking heavily for days and at times an occasional strong glow at night. The Taftan volcanism age ranges from 6.95 to 0.7 Ma based on K-Ar method by Biabangard and Moradian, (2008). The major rock composition is Andesitic of Taftan Volcano (<https://en.wikipedia.org>).

The Bazo volcanic field is in the north-west direction of the Bazman volcanic fields. Bazo is considered to be the extension of the East Shahrvaran volcanic fields. This volcanic field has four volcanic centers viz. Kuh-e-Lurian, Kuh-e-Som, Kuh-e-za-e-Kuchak and Kuh-e-za-e-Bozorg. All these centers contain cinder cones, pyroclastic deposits and lava flows.

1.2 Scope of the Thesis

We chose the Taftan and Bazman volcanic region, Iran, as our main study area (Fig. 1.2). In this MS-Thesis we strive to find the state of the stratovolcanoes in this region, using Geophysics, Petrology and Geochemistry. The geophysics will help in finding the depth profile, Petrological studies will give evidence of the processes that happened in the past, and Geochemical analysis will provide details on the past chemical changes happened. Using the information from all three, we try to comment on the nature of volcanism and subduction.

1.3 Volcanic Rocks

In Bazman most rocks are Andesitic-dacitic. Andesite is an extrusive igneous volcanic rock, having a composition between Rhyolite and basalt. Andesite rock forms when magma erupted on surface crystallizes rapidly. As the crystallization is fast, the grain sizes are small. This volcanic rock is mostly found in the lava flows of stratovolcanoes.

Dacite is also an extrusive igneous rock with an intermediate composition between Rhyolite and andesite. It is mostly found above subduction where a younger oceanic plate has subducted below. (<https://geology.com/rocks.shtml>)

Taftan is mainly andesitic in nature. It also has ignimbrite and pyroclastic deposits. Ignimbrite is a hardened igneous rock which is composed of material ejected during a volcanic eruption. Ignimbrite is mostly formed from pumice dominated pyroclastic flow. (https://flexiblelearning.auckland.ac.nz/rocks_minerals.html). Most of the deposits in Taftan are reworked materials due to erosion and weathering.

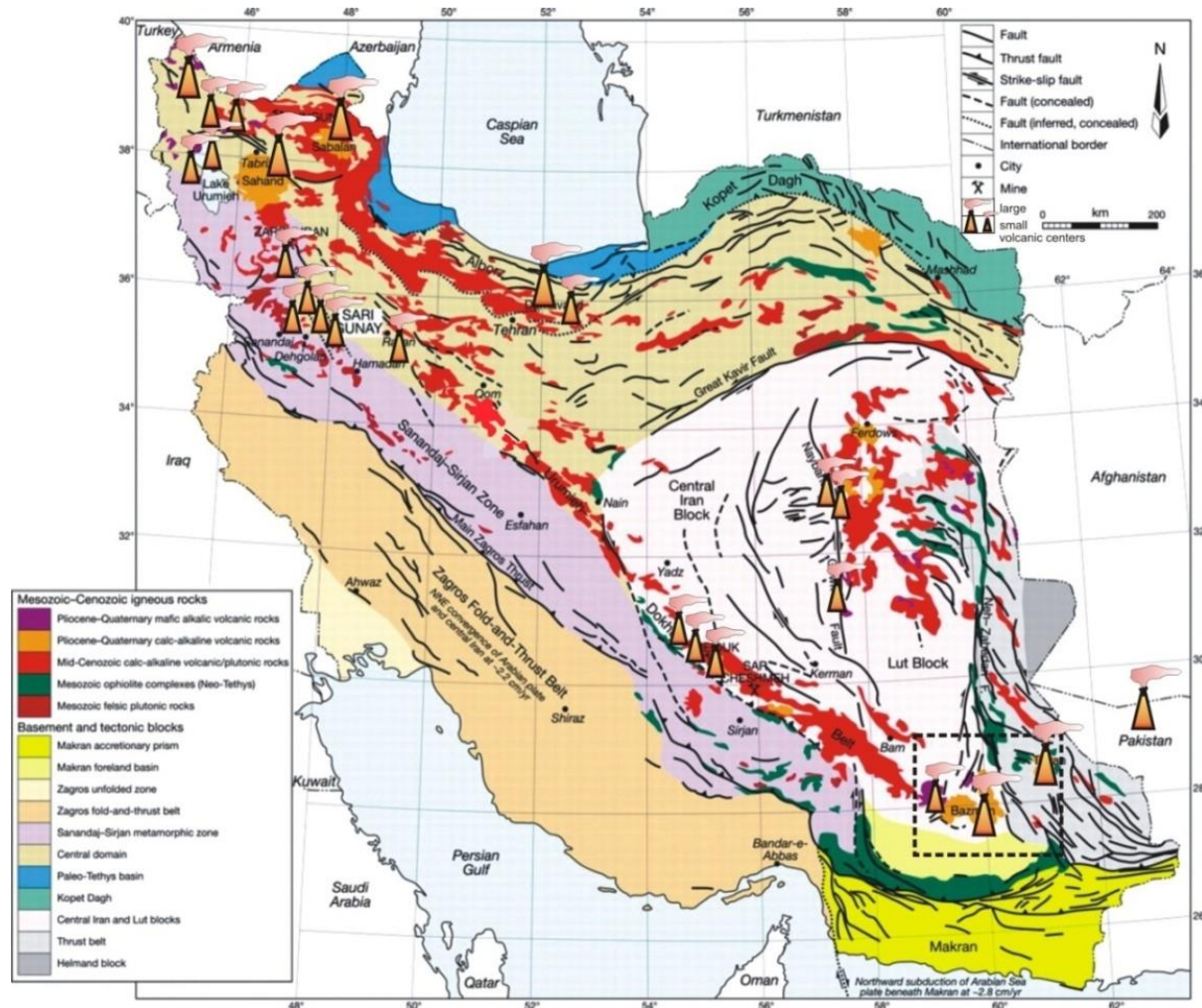
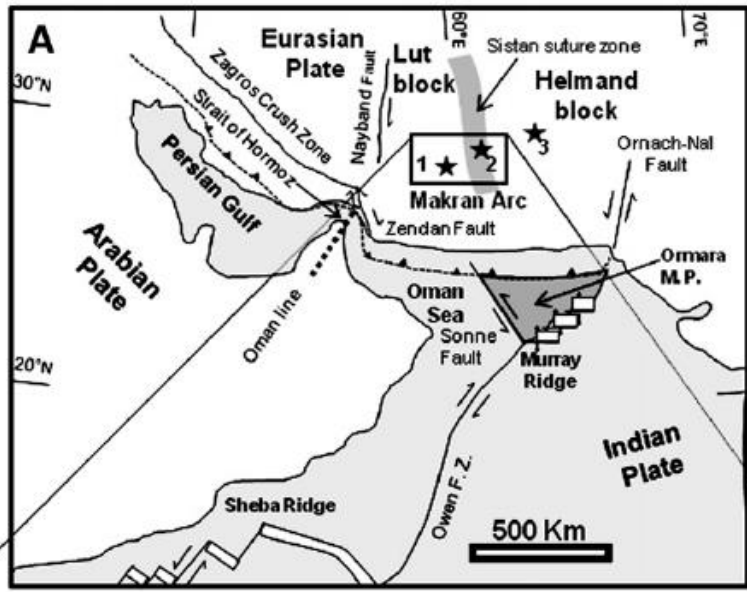


Fig. 1.1: Geological map of Iran showing major volcanoes (modified after Geological Survey & Mineral Exploration of Iran, 2005; (Richard et al., 2006).

1.4 Objectives of the study

The main objectives of this study:

- A. Identifying and documenting the various volcanic features like volcanic cone, crater and pyroclastic products of the Kuh-e-Taftan and Kuh-e-Bazman volcanic site.
- B. Performing the petrography, geochemistry (major oxide and trace element) of the collected rock samples and study the generated cross-section profiles of the study area.
- C. Understanding the nature of volcanism, relate it to the regional subduction and comment on the petrogenesis of volcanic rock of Kuh-e-Taftan and Kuh-e-Bazman.



Sistan-Baluchestan volcanic segment
 bazman and taftan volcanoes along with the abu fazal crater segment and kuh-e-za-kuchak and subsidiary fissures marked in white

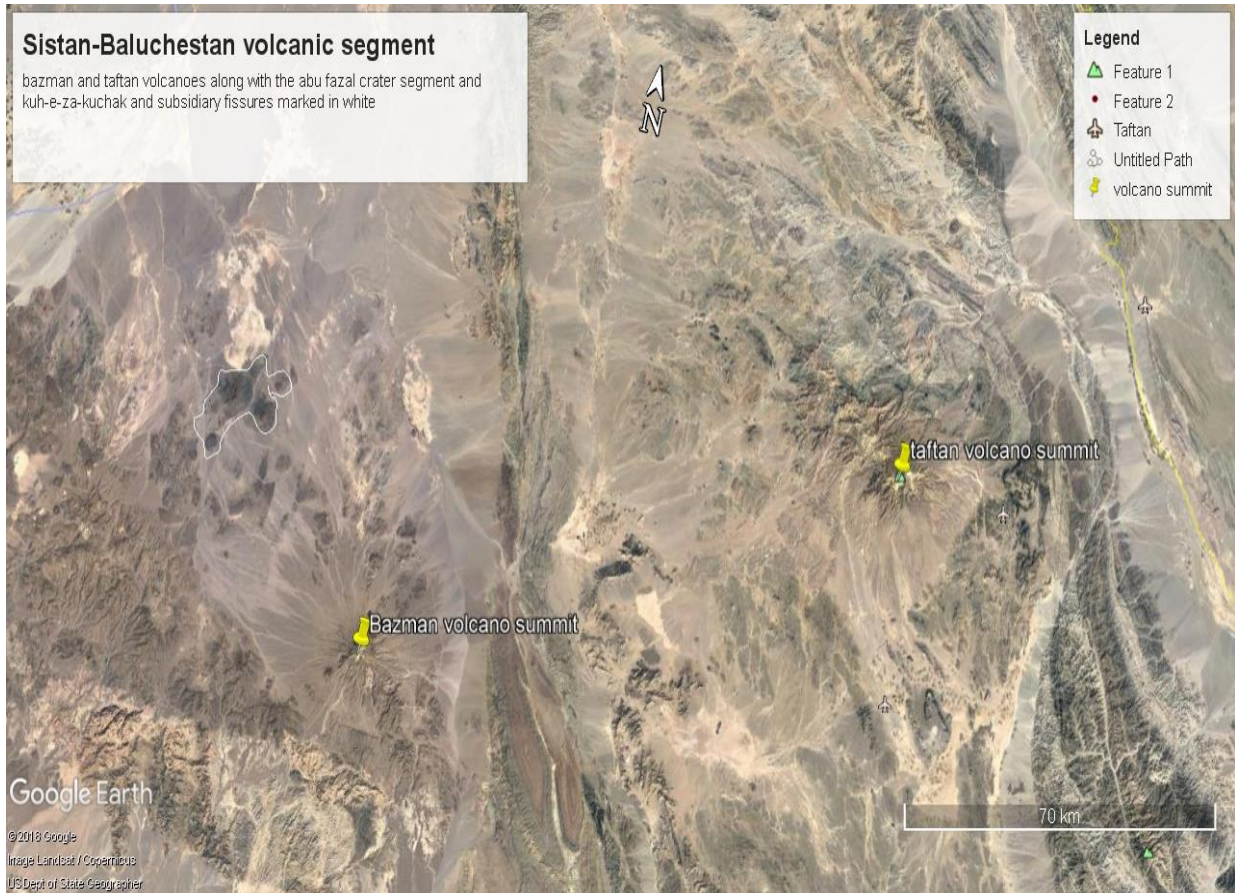


Fig. 1.2: Google Earth image of the Bazman and Taftan volcanic fields, Sistan and Baluchestan province, Iran.

2. MATERIALS AND METHODS

2.1 Literature work

The literature of the area under study was compiled from the libraries of the Sistan and Baluchestan University, Zahedan Iran and Savitribai Phule Pune, Pune India, etc. Most of the relevant material required for carrying out this study was obtained from the internet. The geological map of Iran was taken from the Geological Survey of Iran.

2.2 Field Visit and Rock Sampling

The fieldwork and rock sample collection of andesite-rhyolite lavas, pumice and volcanic ash from Taftan (Fig. 2.1) and Bazman (Fig. 2.2) has been undertaken by the supervisor Dr Raymond Duraiswami and his PhD student Mr Mohammad Noor Sephai. The rock samples were brought back to the Savitribai Phule Pune University for further analysis. Collected rock samples were used for preparing thin sections for petrographic studies and preparing powders for geochemical analyses.

2.3 Sample preparation for Petrography and geochemical analysis

2.3.1 Thin section preparation

Previously collected rock samples were cut and sent for the thin section preparation. The selected rocks were sent to Continental Instruments, Lucknow for Thin section Preparation.

2.3.2 Powdering rock samples for geochemical analysis

The rock samples were powdered using agate motor. Small pieces of each sample (~100 gm) were broken, rinsed several times with distilled water and were hand-ground in an agate mortar and pestle (Fig. 2.3). Agate motor was thoroughly washed and dried in a hot oven after powdering every rock. The consistency of powdered rock should be the same as of talcum powder. A total of 12 rock samples were grounded for the XRF (major oxides) and ICPMS (trace/REE) analysis.



Fig. 2.1: Field photograph of Taftan stratovolcano. (Credits- Mr Noor Mohammad)



Fig 2.2 Field photograph of Bazman stratovolcano (Credits- Mr Noor Mohammad)



Fig. 2.3: Procedure of powdering rocks using hand agate motor

2.4 Petrographic Study

The thin sections of rock were observed under a petrological/polarising microscope (Fig. 2.4). A total of 15 slides were selected for petrographic studies.



Fig 2.4: The above image shows a thin-section slide and the petrological microscope

2.5 Plotting Earthquake Distribution for the study area

The Earthquake Data of the area under study was systematized. Using QGIS, the data from IRIS and EHB was used for plotting the earthquake distribution. The distribution of the earthquake was plotted using the data from 2006 to 2017. The depth was from 0-100 km, and the magnitude was from 3.5-10. Evaluation of the previously plotted earthquake distribution has been completed.

2.6 Geochemical analysis

2.6.1 Acid Dissolution

0.5 gm of powdered sample was weighed using a weighing machine and transferred to a clean and dried Teflon beaker. Separately an acid mixture of 3:1 HCl and HNO₃ was prepared in a glass cylinder. After weighing all samples, 10ml of the prepared acid mixture was added to each Teflon beaker. After adding acid, the samples were kept in a hot oven to react and dry completely. After some hours/days the sample is reduced to a clean slurry we then add the borax solution to ensure there is no unreacted silica. The sample is now filtered using Whatman filter paper (size) and is allowed to drip in a conical flask (Fig. 2.5). Do not disturb the solution until it's filtered completely. Using distilled water, the solution is made 100 ml and then transferred to a clean bottle for ICPMS analysis.



Fig 2.5: The above image shows filtering of dissolved rock samples for ICPMS analysis

2.6.2 XRF sample loading

Two samples from Taftan, three from Bazman and four from Kuh-e-Som region were selected for the analysis using the X-ray Fluorescence technique for the major oxide analyses and trace element analysis at the Department of Geology, SPPU, Pune. From 4 grams of sample and 0.7 grams of wax, the powder pellets were made. Ten tone of pressure was applied to make pellets. The samples were analyzed using SPECTRO ED-XRF equipment. Using known standards calibration for both major oxides and trace

elements was done. The major oxide analyses were used to calculate the normative mineral compositions using SINCLAS program of Verma et al. (2002). The programme gives a rock name, fixes the Fe_2O_3 : FeO ratio and then calculates the norm. The major oxide and normative mineralogy obtained were used to classify the rock. The major oxides are given in Table 1, and the trace elements are presented in Table 2.

2.7 Making Cross-section maps using Earthquake data

Using the Earthquake data of the study area, auto-correlation and cross-correlation and inversion of the data was done. The final image of the velocity v/s depth profile of the study area was developed with the help of Prof Shyam S Rai and his PhD student Gokul Saha.

3. RESULTS

3.1 Thin-section Observations

Thin section study is an important part of studying the minerals and rocks without any physical destruction. Thin section study has proved to be helpful by using the textural information and the estimate of chemical composition. Small pieces of evidence from microscopy study can be helpful to know about the formation of the material/mineral.

3.1.1 Textural study and Petrography

This study was carried out at the Optical Laboratory, Department of Geology, SPPU, Pune. Nikon D330 microscope with the photographic attachment was used for studying rock samples from Taftan, Bazman and Bazo. Textural and mineralogical study of fifteen slides was carried out.

3.1.1.1 Petrography of Quenched Pyroxene (Sample ID: TAF-1)

The rock has a variety of medium and large crystals. The crystal at the centre is euhedral. Erratic Plagioclase needles are widely dispersed around the big pyroxene crystal. This dark coloured rock shows a porphyritic texture. The Pyroxene crystal shows quenched texture which signifies the presence of volatiles. The pyroxene crystal also shows a reaction rim where pargasitic amphibole developed. Refer Fig. 3.1

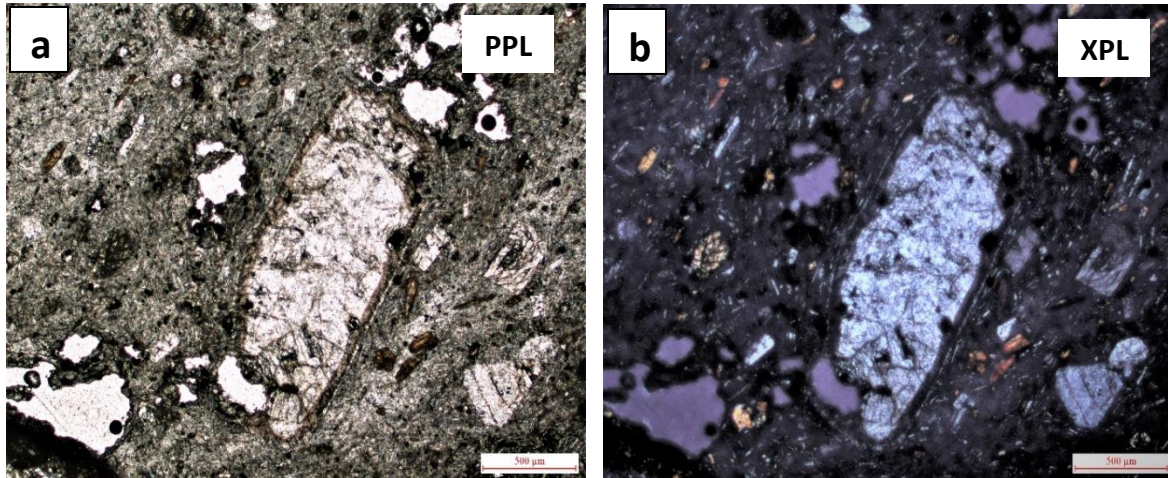
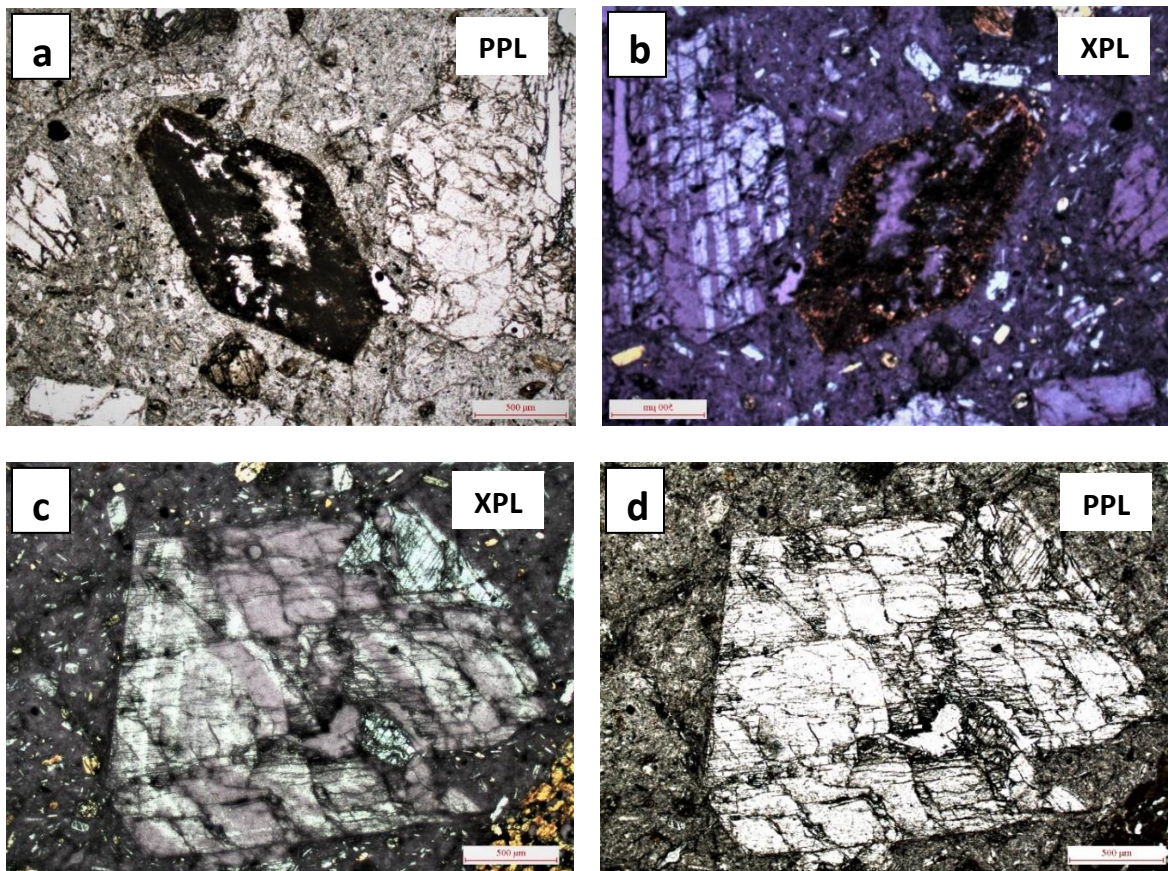


Fig 3.1: Thin section slide showing Pyroxene crystal with inclusions and thin reaction rim

3.1.1.2 Petrography of sieved Pyroxene and fretted and strained Plagioclase (Sample ID: TAF-2)



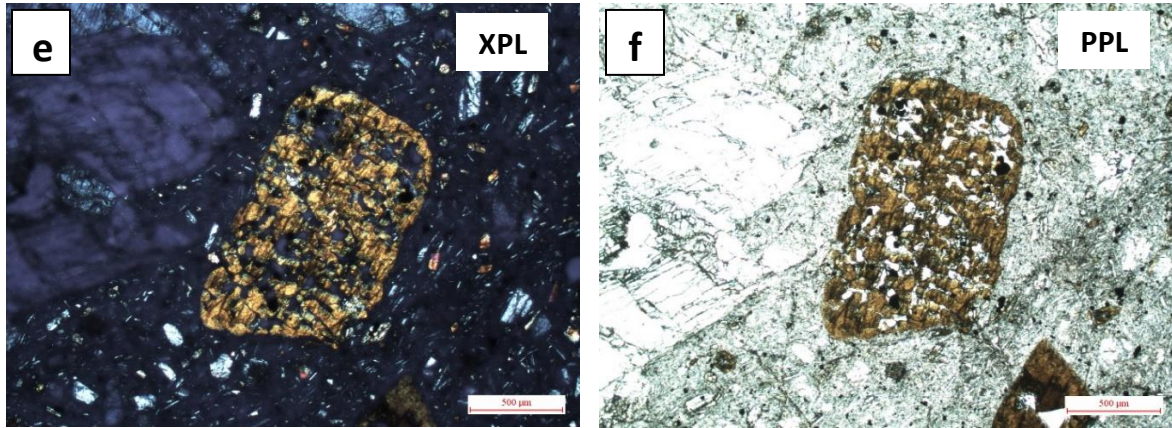
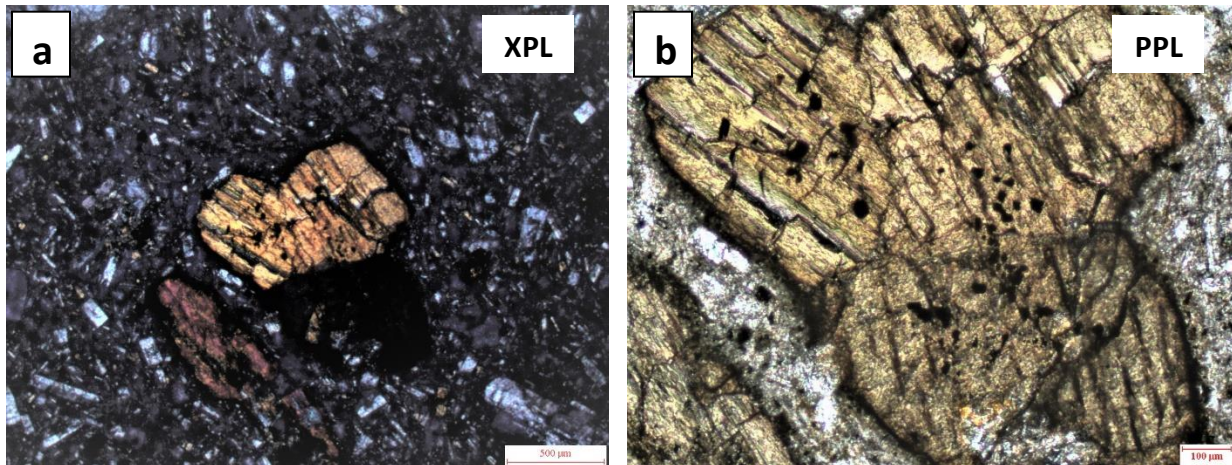


Fig 3.2: Thin section slide showing reabsorbed Pyroxene crystal

This rock specimen shows glassy texture with groundmass consisting microphenocrysts of pyroxene and Plagioclase minerals. Big Pyroxene crystals are breaking into smaller pieces. It is a crystal ignimbrite. The sieved Pyroxene shows the presence of gas or indication of explosive volcanoes. The sieved Pyroxene shows a porphyritic texture. Above shown pyroxene crystals are euhedral in shape. Few Zoned plagioclases are also observed with sharp and some altered edges. The shown zoned Plagioclase is euhedral showing porphyritic texture. Refer Fig. 3.2

3.1.1.3 Petrography of Prismatic Pyroxene and zoned Plagioclase (Sample ID: TAF-4)



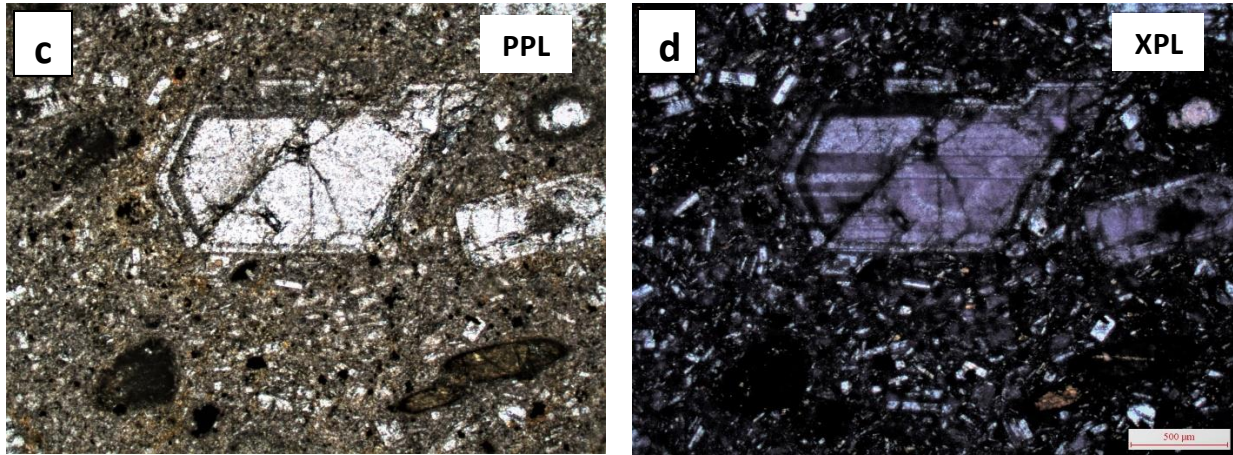
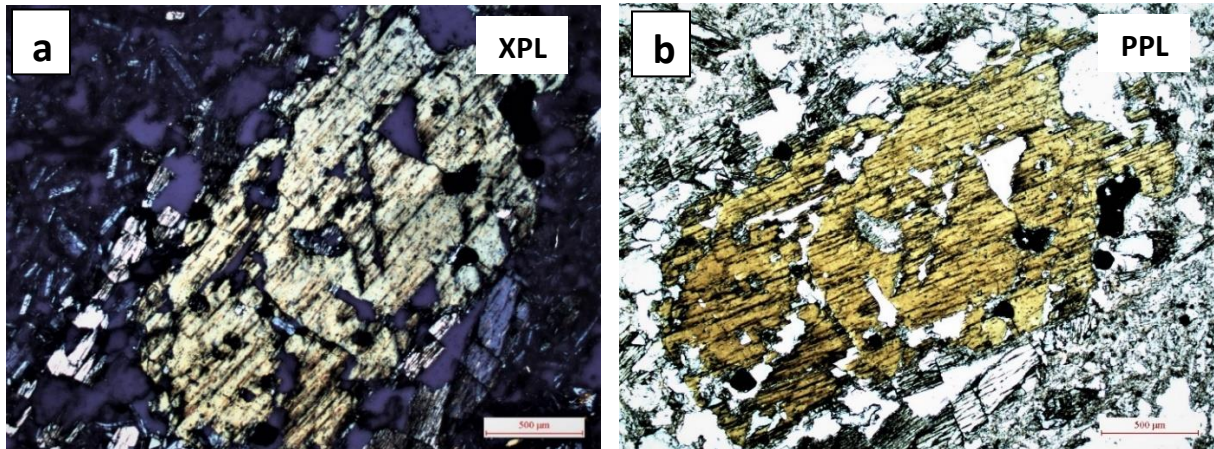


Fig 3.3: Thin section slide showing prismatic Pyroxene and zoned Plagioclase crystal

This thin section shows euhedral Plagioclase mineral with zoning and alteration. The slide also indicates prismatic subhedral pyroxenes. Both the mineral shows porphyritic textures. Both the images have plagioclase and pyroxenes microphenocrysts in the groundmass. These minerals are randomly oriented in the sample with no directionality. The pyroxene mineral shows high pleochroism. Refer Fig. 3.3

3.1.1.4 Petrography of shattered Pyroxene and zoned Plagioclase (Sample ID: BAZ 20/17)



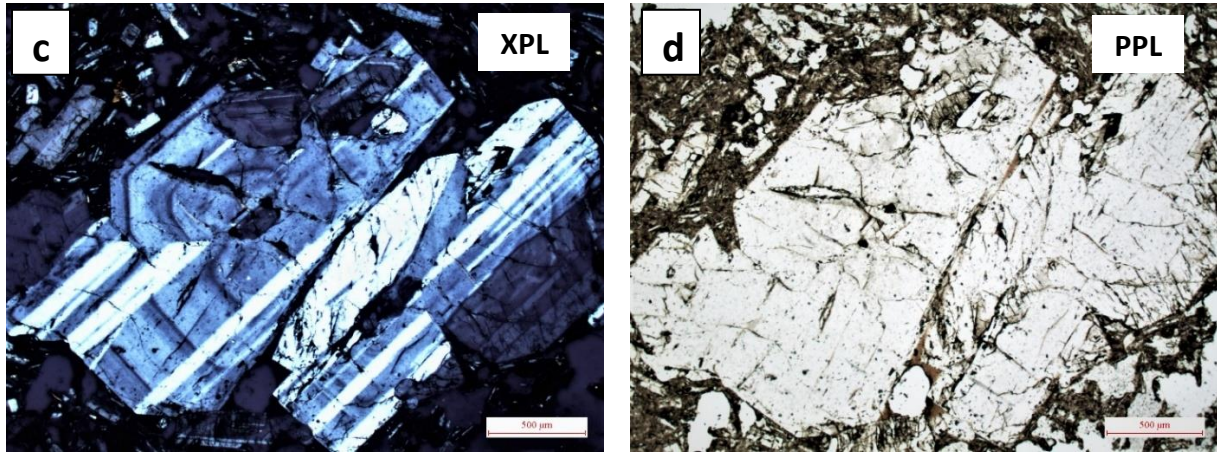


Fig 3.4: Thin section slide showing shattered Pyroxene and zoned Plagioclase crystal

This specimen contains shattered subhedral to anhedral pyroxene mineral crystal. It also contains opaque phenocrysts of magnetite mineral. A cleavage plane (slightly distorted) is observed parallel to the length of the crystal. Very beautiful zoned and twinned plagioclase mineral is observed. The crystal is euhedral in shape. In the above picture, all the plagioclases are glued together, showing glomeroporphyritic texture. Refer Fig. 3.4

3.1.1.5 Petrography of reabsorbed Pyroxene and strained vesicles (Sample ID: BAZ 25/17)

In this thin section, the Plagioclase is strictly restricted to groundmass. Plagioclase needles in groundmass are randomly dispersed. The slide is filled with many vesicles. Most of the vesicles are deformed; this could be because of the stress they underwent. The Pyroxene in c and d shows the beginning of alteration in it. The groundmass is attacking the Pyroxene and consuming it. Due to this, the embayment structure is formed. Similarly, in e and f reabsorption of euhedral to subhedral Pyroxene has taken place. Due to reabsorption, the euhedral boundaries are incomplete. Refer Fig. 3.5

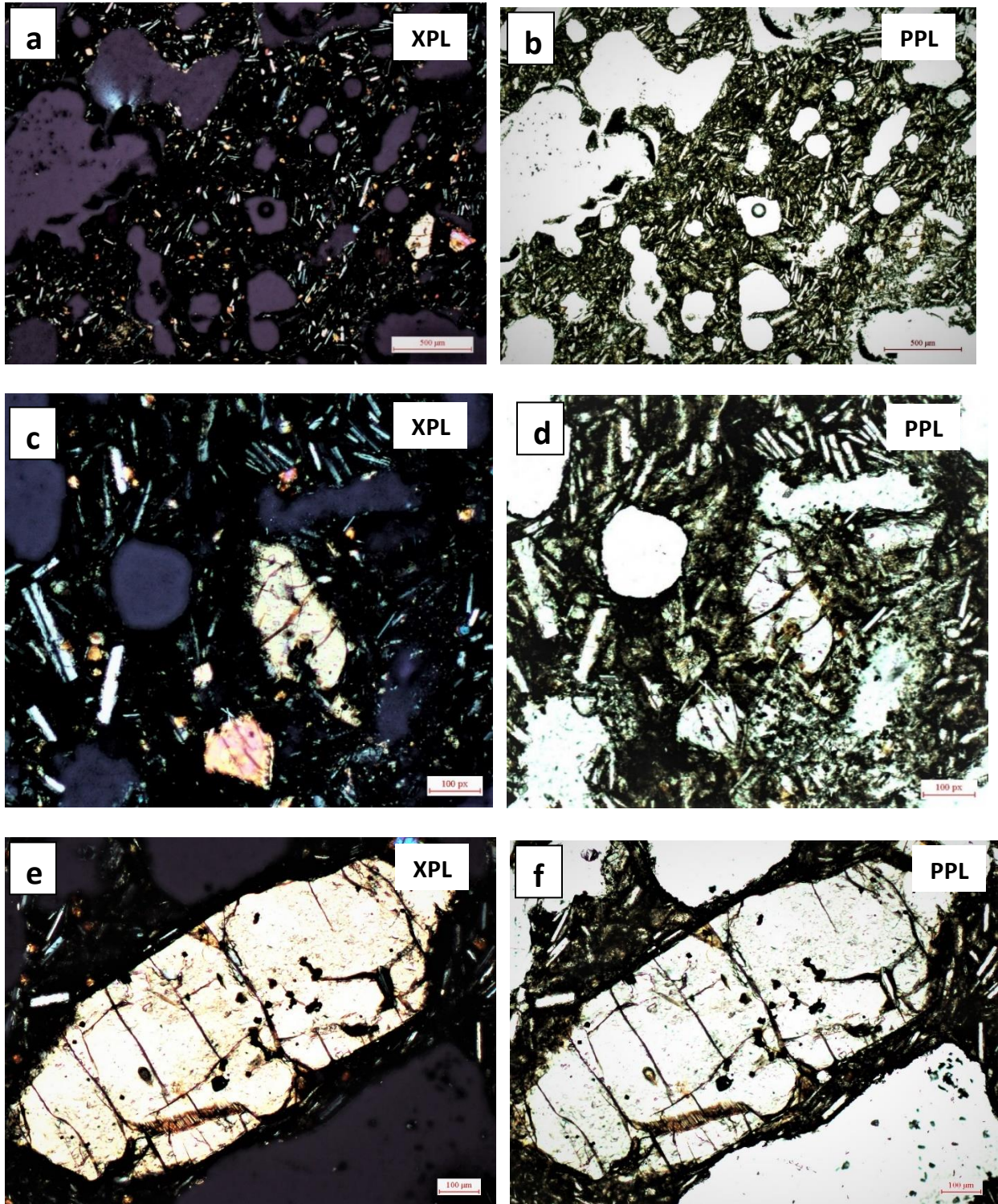


Fig 3.5: Thin section slide showing strained vesicles and reabsorbed pyroxene crystal

3.1.1.6 Petrography of altered Pyroxene (Sample ID: BAZ 9/17)

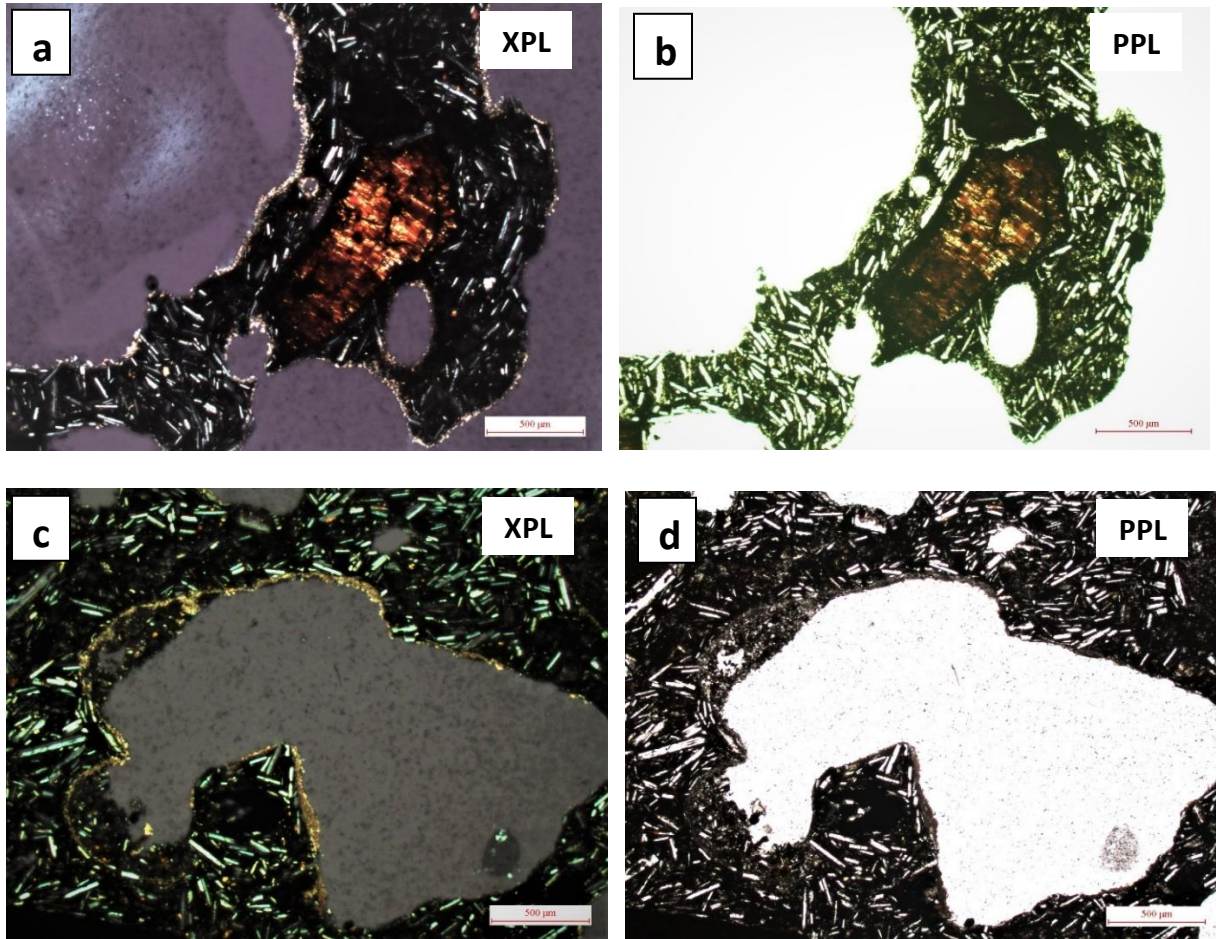


Fig 3.6: Thin section slide showing altered Pyroxene and mesostatic glass needles in groundmass

This specimen shows euhedral-subhedral pyroxene crystal which has undergone deuteric alteration. The dark colour of Pyroxene signifies it has undergone oxidation. The glass in the groundmass is also altered. The glass needles are randomly oriented throughout the thin section. In c and d crystal nucleation is observed. This crystal nucleation is seen in every vesicle lining. Refer Fig. 3.6

3.1.1.7 Petrography of deformed vesicles (Sample ID: BAZ 24/17)

In this thin section, the vesicles are mostly circular. Some deformation is seen in vesicles, but it's smaller than the BAZ 25/17 slide. This slide mostly has glass and vesicles, which is distributed all over the slide. We see segregation vesicles. Glass dripped into vesicles, but the vesicle didn't burst. Therefore glass didn't cool immediately; it got time to cool. Refer Fig. 3.7

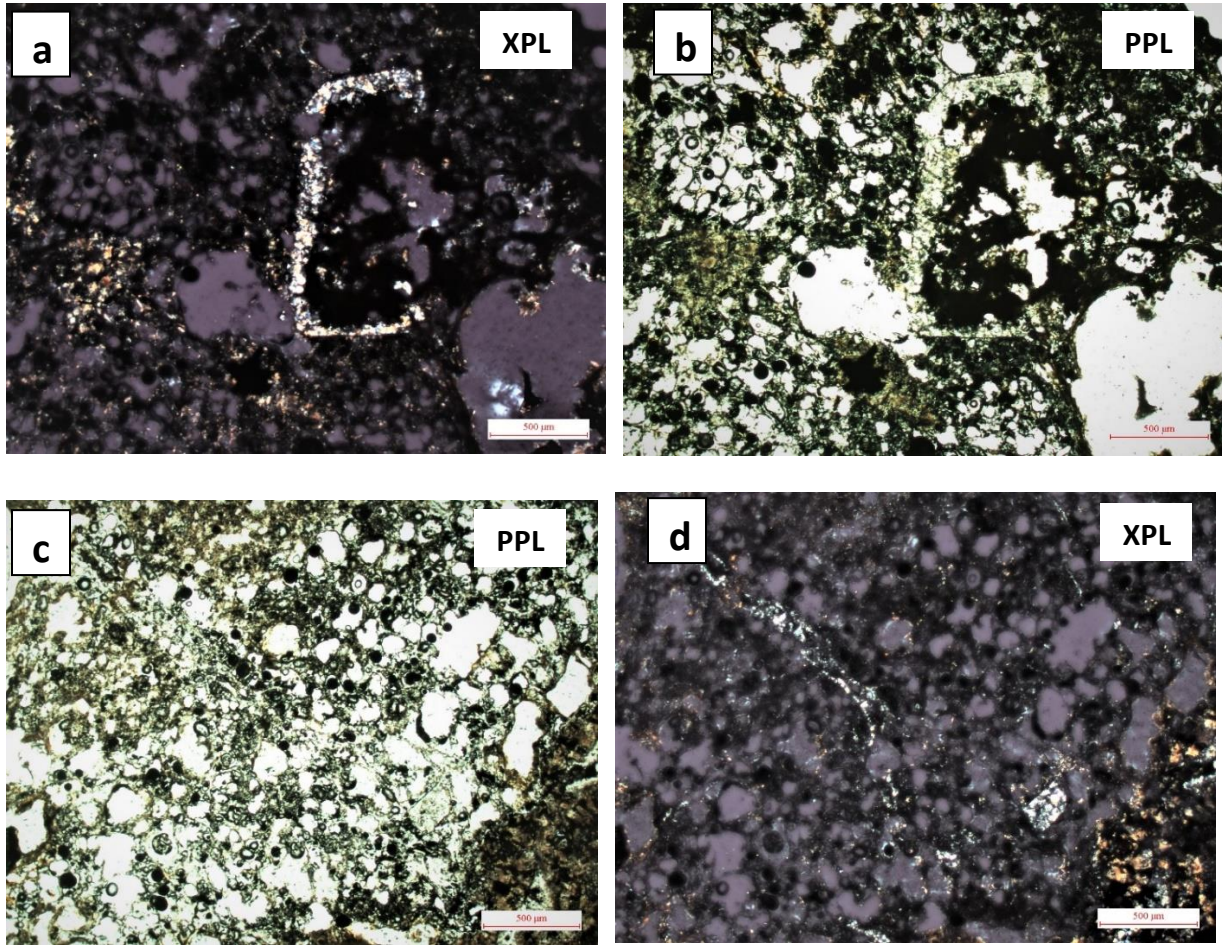
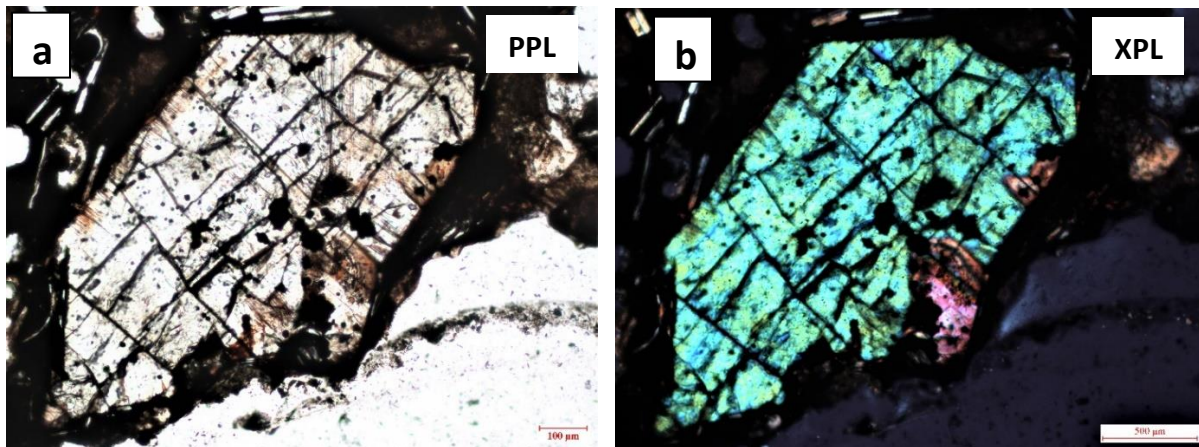


Fig 3.7: Thin section slide showing deformed spherical vesicles

3.1.1.8 Petrography of altered skeletal Pyroxene (Sample ID: BAZ 22/17)

This specimen shows alteration features. Skeletal Pyroxene is seen. Due to the paucity of minerals, the Pyroxene is reabsorbed. Deuteric alteration of pyroxene crystal has taken place Refer to Fig. 3.8



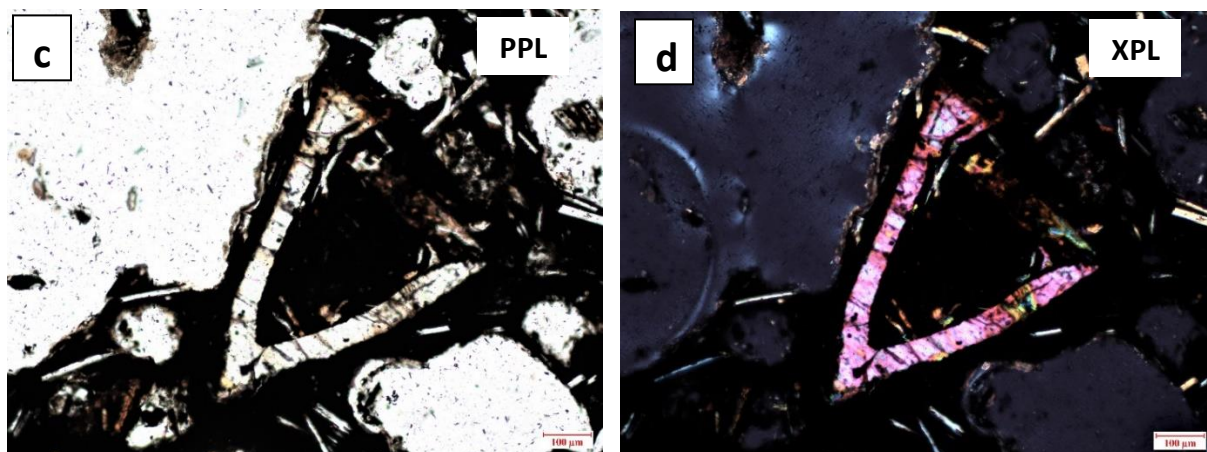


Fig 3.8: Thin section slide showing skeletal Pyroxene

3.2 Results of Geochemical analysis

3.2.1 Major oxides analysis

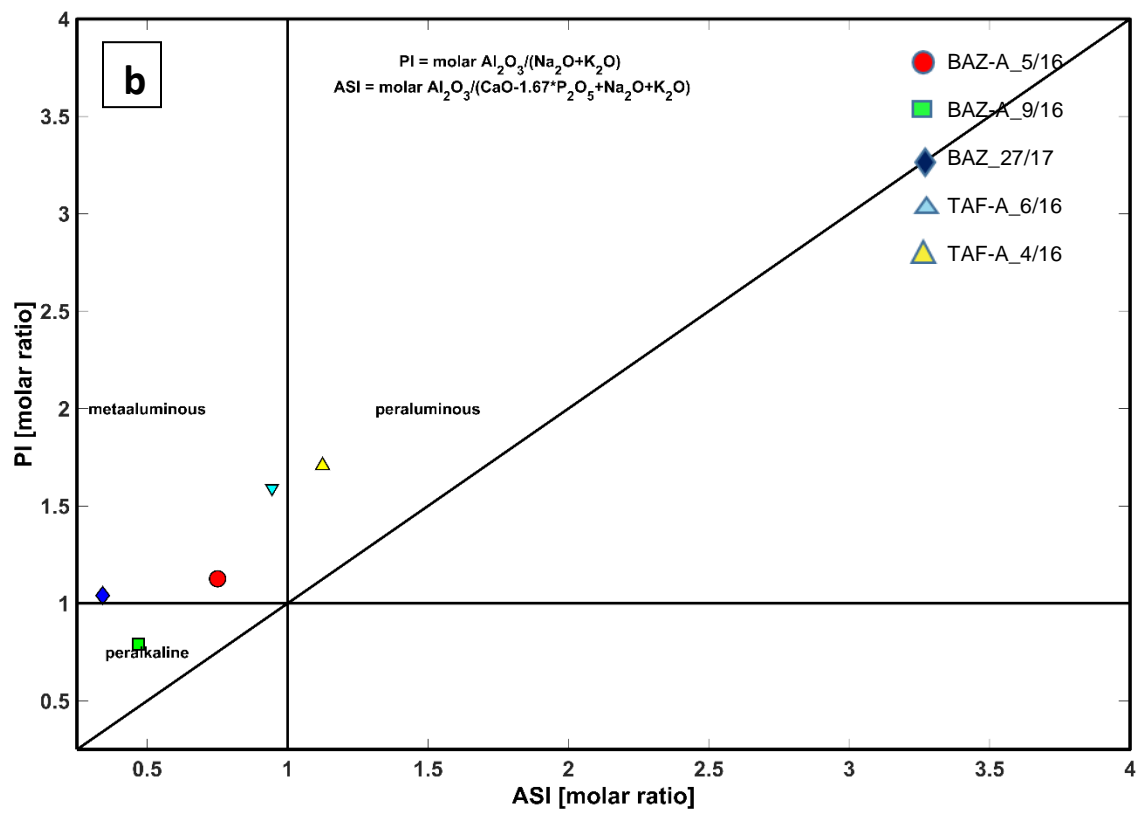
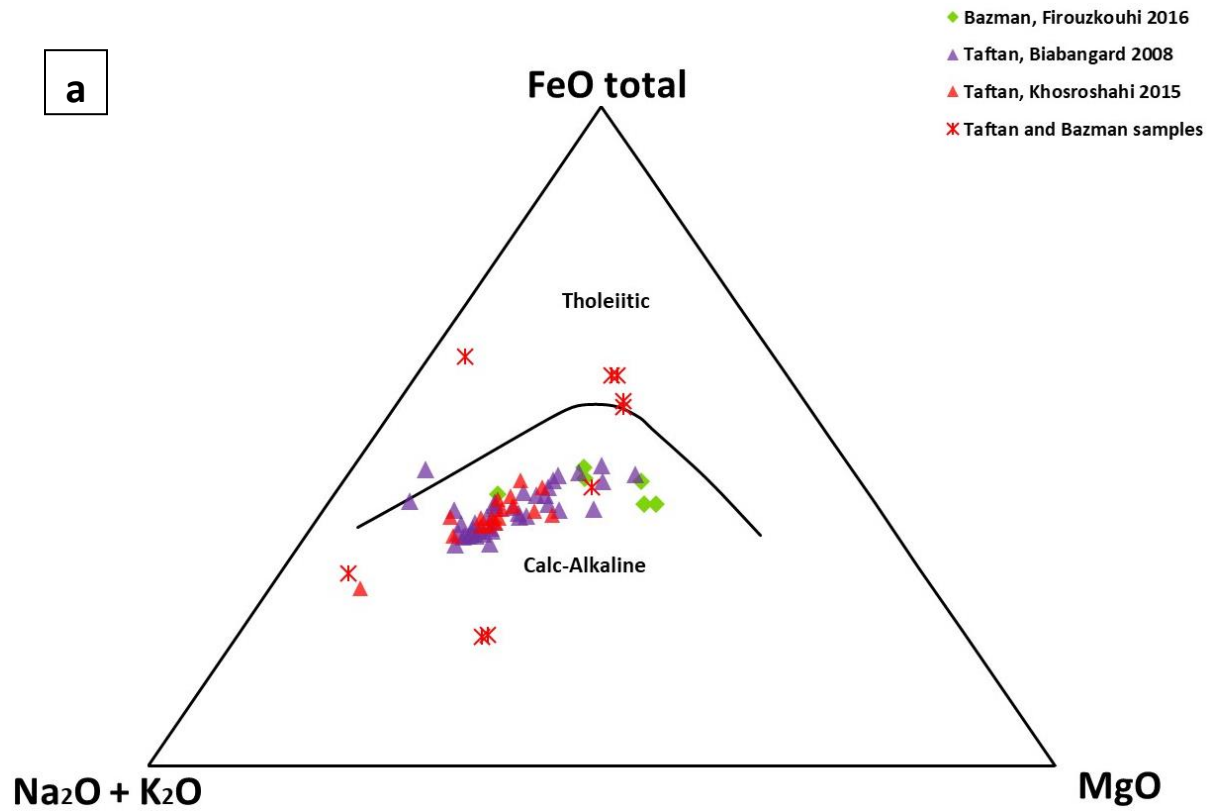
The major oxide study results for five samples from Bazman and Taftan is given below in Table 1.

Table 1: Major oxide (wt.%) and CIPW norms of rocks from Kuh-e-Som (after Saurajith Sahoo, 2019) and Bazman and Taftan stratovolcanoes (present study).

Locality	Kuh-e-Som				Bazman			Taftan	
Sample	BM 1/16	BM 2/16	OBS- NEW	OBS- OLD	BAZ/ A5/16	BAZ/ A9/16	BAZ 27/17	TAF- A4/16	TAF- A6/16
Comp.	B, subal	B, subal	B, subal	B, subal	A	T	TB, Haw	R, peral	R, peral
SiO ₂	49.01	48.37	49.20	49.50	61.54	63.34	48.77	79.84	77.17
TiO ₂	0.91	0.87	0.88	0.87	0.51	0.57	1.19	1.12	0.90
Al ₂ O ₃	15.67	14.99	16.38	16.06	15.78	15.44	15.31	5.43	5.00
FeOT	9.34	9.05	9.62	9.65	11.81	4.11	9.31	0.68	0.69
MnO	0.15	0.16	0.15	0.15	0.07	0.08	0.16	0.01	0.01
MgO	4.17	4.21	3.50	3.62	0.75	1.05	6.13	0.94	0.96
CaO	12.46	12.64	12.58	12.56	2.95	5.60	12.52	0.72	0.93
Na ₂ O	2.35	2.36	2.33	2.29	4.99	7.23	5.68	3.01	2.01
K ₂ O	0.96	0.98	0.78	0.72	1.47	1.69	0.95	1.86	1.83
P ₂ O ₅	0.22	0.22	0.20	0.20	0.14	0.17	0.28	0.09	0.12
Total	95.24	94.26	95.62	95.62	100.0	99.28	100.3	93.70	89.62
					1		0		
SiO ₂ adj	51.37	51.46	51.37	51.68	61.34	63.71	48.52	85.19	86.09
TiO ₂ adj	0.95	0.92	0.92	0.93	0.51	0.57	1.18	1.20	1.00
Al ₂ O ₃ adj	16.43	15.95	17.10	16.77	15.73	15.53	15.23	5.79	5.58
Fe ₂ O ₃ adj	1.66	1.63	1.70	1.71	3.13	1.43	2.19	0.25	0.27
FeOadj	8.29	8.16	8.52	8.54	8.95	2.85	7.29	0.50	0.53

MnOadj	0.16	0.17	0.15	0.15	0.07	0.08	0.16	0.01	0.01
MgOadj	4.37	4.48	3.66	3.78	0.75	1.06	6.10	1.00	1.07
CaOadj	13.06	13.44	13.13	13.11	2.94	5.63	12.46	0.77	1.04
Na ₂ Oadj	2.46	2.51	2.43	2.39	4.97	7.27	5.65	3.21	2.24
K ₂ Oadj	1.01	1.04	0.82	0.76	1.47	1.70	0.95	1.99	2.04
P ₂ O ₅ adj	0.23	0.24	0.21	0.21	0.14	0.17	0.28	0.10	0.13
Q	0.64	0.16	1.78	2.47	13.80	5.03	0.00	61.27	63.36
Or	5.96	6.17	4.82	4.46	8.66	10.05	5.59	11.73	12.06
Ab	20.80	21.24	20.54	20.25	42.09	61.53	13.67	18.75	17.32
An	30.82	29.17	33.35	32.78	13.68	4.71	13.40	0.00	0.00
Ne	--	--	--	--	--	--	18.50	--	--
Di	27.01	29.87	25.49	25.88	0.00	15.12	38.00	0.78	2.24
Hy	10.03	8.73	9.32	9.46	15.00	0.00	0.00	2.14	1.63
Ol							4.78		
Mt	2.41	2.37	2.47	2.48	4.54	2.07	3.17	0.00	0.00
Il	1.81	1.75	1.75	1.76	0.97	1.09	2.25	1.08	1.15
Ap	0.53	0.55	0.48	0.47	0.32	0.40	0.65	0.22	0.31
Sph	--	--	--	--	--	1.54	0.99	--	--
Ns	--	--	--	--	--	1.77	0.18	--	--
Mg#	48.46	49.49	43.37	44.08	12.96	39.77	59.85	78.13	78.24
FeOT/MgO	2.24	2.15	2.75	2.67	15.75	3.91	1.52	0.72	0.72
Salic	58.22	56.74	60.49	59.96	78.22	81.32	32.66	91.75	92.74
Femic	27.70	28.01	24.90	25.42	20.51	14.96	48.20	4.00	5.01
Cl	63.11	64.78	60.56	60.85	14.98	16.95	68.41	3.18	5.97
DI	27.40	27.56	27.14	27.18	64.54	76.61	37.75	91.75	92.74
SI	24.58	25.15	21.37	21.99	3.88	7.38	27.50	14.43	17.41
AR	1.27	1.28	1.24	1.24	2.05	2.47	1.63	8.61	4.68

In general, the samples from Bazman have a SiO₂ ranging from 48 to 70 wt. %, MgO from 0.7 to 6 wt. %, TiO₂ from 0.5 to 1.2 wt. % and Al₂O₃ with a smaller range from 15.3 to 15.78 wt. % whereas the Taftan samples show a higher range of SiO₂ ranging from 77 to 90 wt. %, MgO from 0.034 to 0.9 wt. %, TiO₂ with a small range from 0.9 to 1.1 wt. % and Al₂O₃ from 5 to 5.4 wt. %.



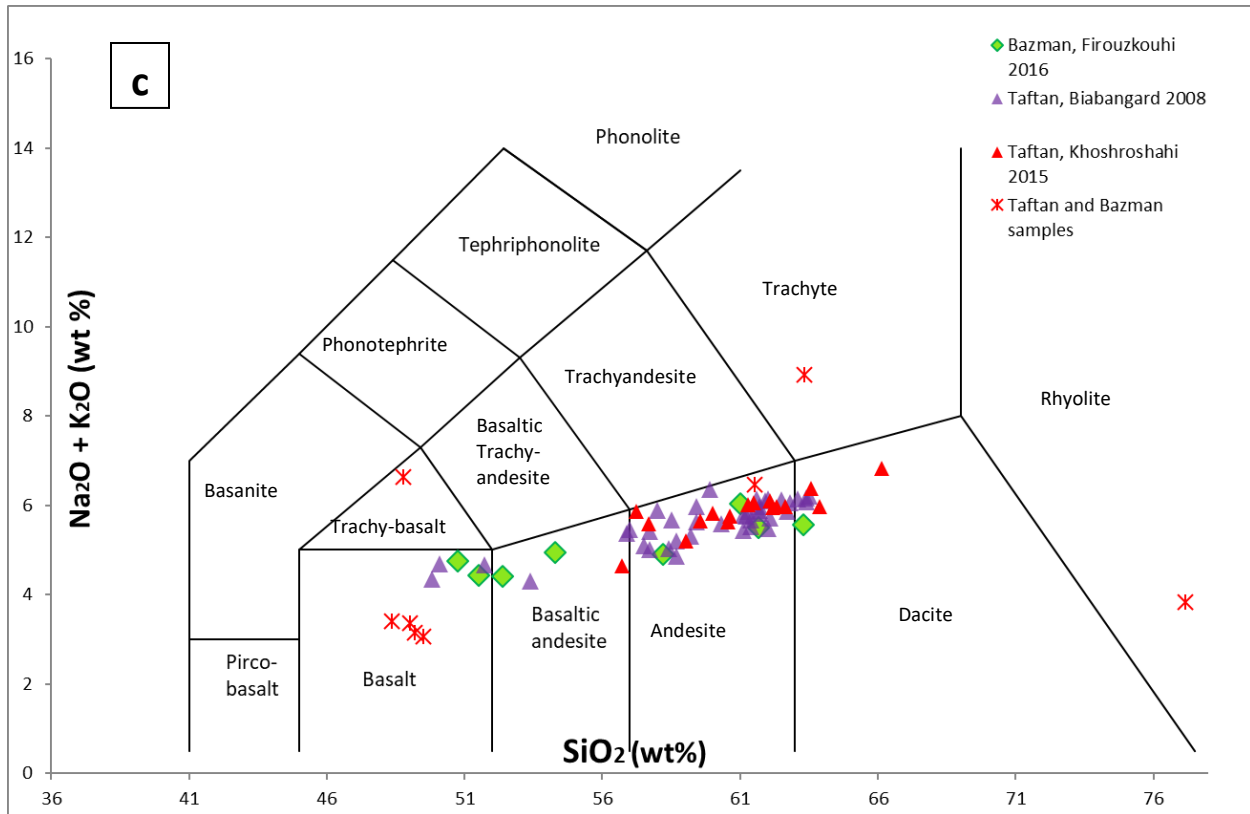


Fig. 3.9: Geochemical plots. (a) AFM diagram (Irvine Baragar et al. 1971) (b) PI vs. ASI (Shand and Shand et al. 1927) (c) $\text{Na}_2\text{O} + \text{K}_2\text{O}$ vs SiO_2 (Middlemost 1994)

The plot **a** shows BAZ 27/17, BAZ-A_9/16, TAF-A_6/16 lie below the calc-alkaline trend line. The TAF-A_4/16 lies on the line joining $\text{Na}_2\text{O} + \text{K}_2\text{O}$ and FeO. The BAZ-A_5/16 lies above the calc-alkaline trend, i.e. in the tholeiitic region but closer towards the $\text{Na}_2\text{O} + \text{K}_2\text{O}$ and FeO line. The Kuh-e-Som samples fall in the tholeiitic region. Rest samples from different published literature are plotted to show a comparison and verify our results.

The plot **b** shows that BAZ/A_9/16 lies in the peralkaline region. Whereas BAZ 27/17, TAF-A_6/16, BAZ-A_5/16 lies in the metaaluminous region. TAF-A_4/16 lies in the peraluminous region.

The plot **c** shows a comparison between previous studies and the samples I analysed. Samples from Taftan and Bazman are plotted.

3.2.2 Trace element analysis

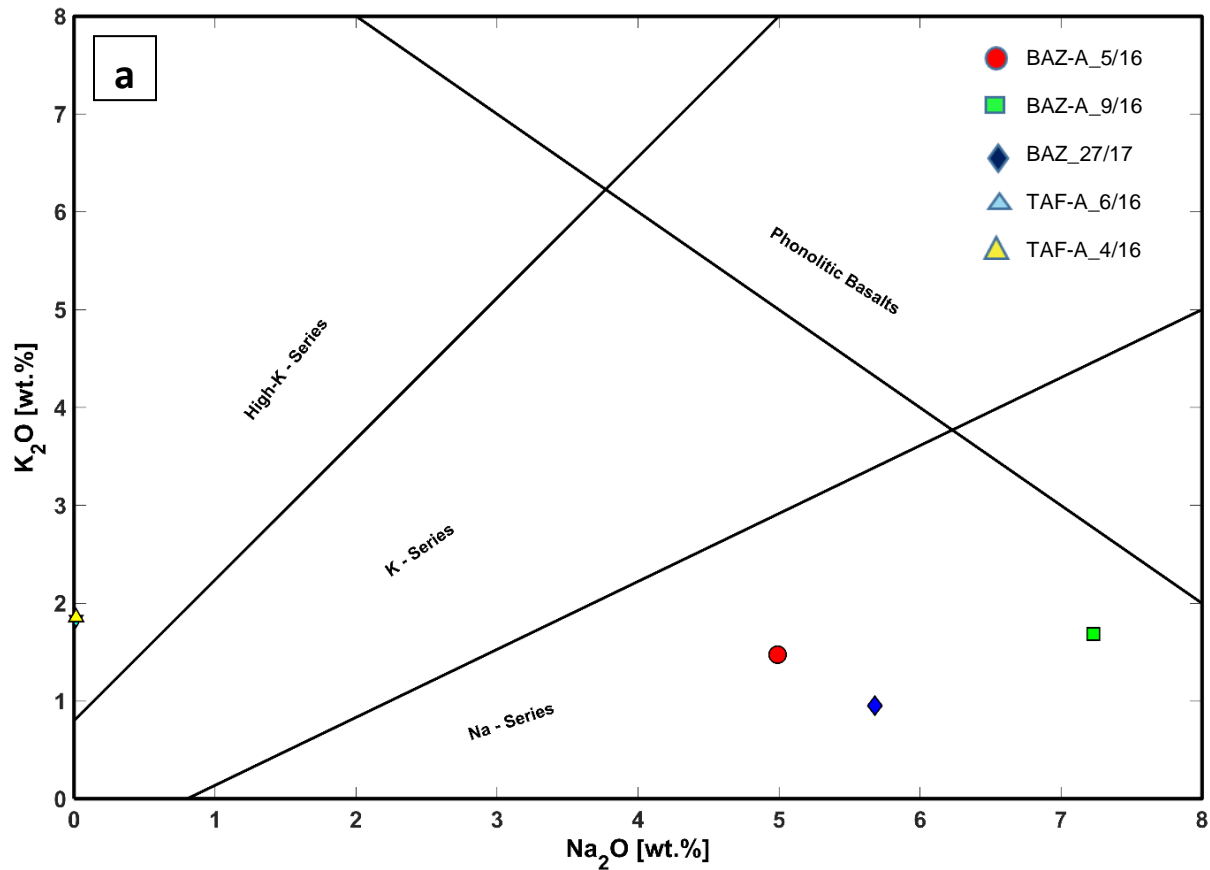
The result of trace element analysis for five samples from Taftan and Bazman is shown below in Table 2.

Table 2: Trace elements (ppm) of rocks from Kuh-e-Som (after Saurajith Sahoo. 2019) and Bazman and Taftan stratovolcanoes (present study). Abbreviations: bdl- below detection level. Abbreviations: B, subalk= basalt sualkaline, A= andesite, T= trachyte, TB= trachy basalt, Haw= Hawaiite, R, subalk= Rhyolite, subalkaline, CI = Crystallization Index; DI = Differentiation Index; SI = Solidification Index; AR = Alkalinity Ratio. Fe₂O₃T = total iron expressed as Fe₂O₃; Mg# = 100 Mg²⁺/(Mg²⁺ + Fe²⁺), atomic; FeOT = total iron expressed as FeO

Localit y	Kuh-e-Som				Bazman			Taftan	
Sampl e	BM 1/16	BM 2/16	OBS- NEW	OBS- OLD	BAZ/ A5/16	BAZ/ A9/16	BAZ 27/17	TAF-A 4/16	TAF-A 6/16
Comp.	B, subal	B, subal	B, subal	B, subal	BAZ/ A5/16	BAZ/ A9/16	BAZ 27/17	TAF- A4/16	TAF- A6/16
S	560	402 2 184	98.5	67.2	1030	155	1327 0	34850	13160 0
Cl	481	7	1146	1754	1883	181	970	799	1720
V	102	115	112	118	32	33	96	1.0	19
Cr	34.6	43.8	35.2	41.4	9.6	7.0	135.4	1.0	1.0
Co	20.6	27.1	42.3	31	11	17.6	28.2	3.0	3.0
Ni	46.5	53.7	53.5	45.5	19.2	17.5	92.6	1.0	2.0
Cu	16.4	40.7	50.6	50.9	25.5	25.2	58.8	5.8	9.7
Zn	81.4	85.8	85.5	89.1	52.3	63.2	89.7	15.4	19.5
Ga	11.2	20.2	22.2	24.8	16.1	18.7	12.1	7.9	8.7
As	bdl	2.3	0.8	bdl	2.6	bdl	bdl	9.0	19.6
Se	0.5	1.1	0.7	0.8	bdl	bdl	bdl	1.6	2.9
Br	3.6	6.6	6.1	7.5	6.3	2.4	3.8	8.2	11.9
Rb	27.4	28.1	18	16.3	43.7	44.2	14.4	96.7	94.2
Sr	629	957	585	582	316.6	423.8	863.5	107.1	103.5
Y	20.1	19.7	19.6	20.0	12.7	15.1	21.9	6.7	7.8
Zr	123	102	117	114	128.8	136.4	112.6	208.7	190.7
Nb	5.6	4.6	3	5.1	5.8	6.1	6.1	15.7	20.4
Mo	3.7	4.2	3.6	4.4	1.9	2.3	3.7	4.1	4.7
Sn	13.7	12.7	6.1	11	9.2	10	6.3	15.6	9.1
Ba	258	364	180	183	245	302	159	434	293
La	28.6	3.3	34.2	17.3	bdl	28.7	bdl	bdl	65
Pb	10.8	9.9	9	10.8	6.1	13	13.9	19.6	14.6
Th	5.0	3.3	2.6	2.9	2.8	8.7	4.0	15.9	15.5
U	6.1	3.7	3.9	4.7	3.2	6.4	4.8	4.6	4.3

For Bazman, the concentration of Cr in the samples ranges from 7-135 ppm, Rb ranges from 14–44 ppm, Sr ranges from 316 to 863 ppm, and Pb varies from 6–14 ppm. The U and Th vary from 3-6 ppm and 2.8-8.7 ppm respectively. V, Co and Ni range from 32-96 ppm, 11-28 ppm and 19-93 ppm respectively. Ba varies from 159-300 ppm.

For Taftan, the concentration of Cr in the samples is less than 1 ppm, Rb ranges from 94-96 ppm, Sr ranges from 103 to 107 ppm, and Pb varies from 14–19 ppm. The U and Th vary from 3-6 ppm and 2.8-8.7 ppm respectively. V, Co and Ni range from 32-96 ppm, 11-28 ppm and 19-93 ppm respectively. Ba varies from 293-434 ppm.



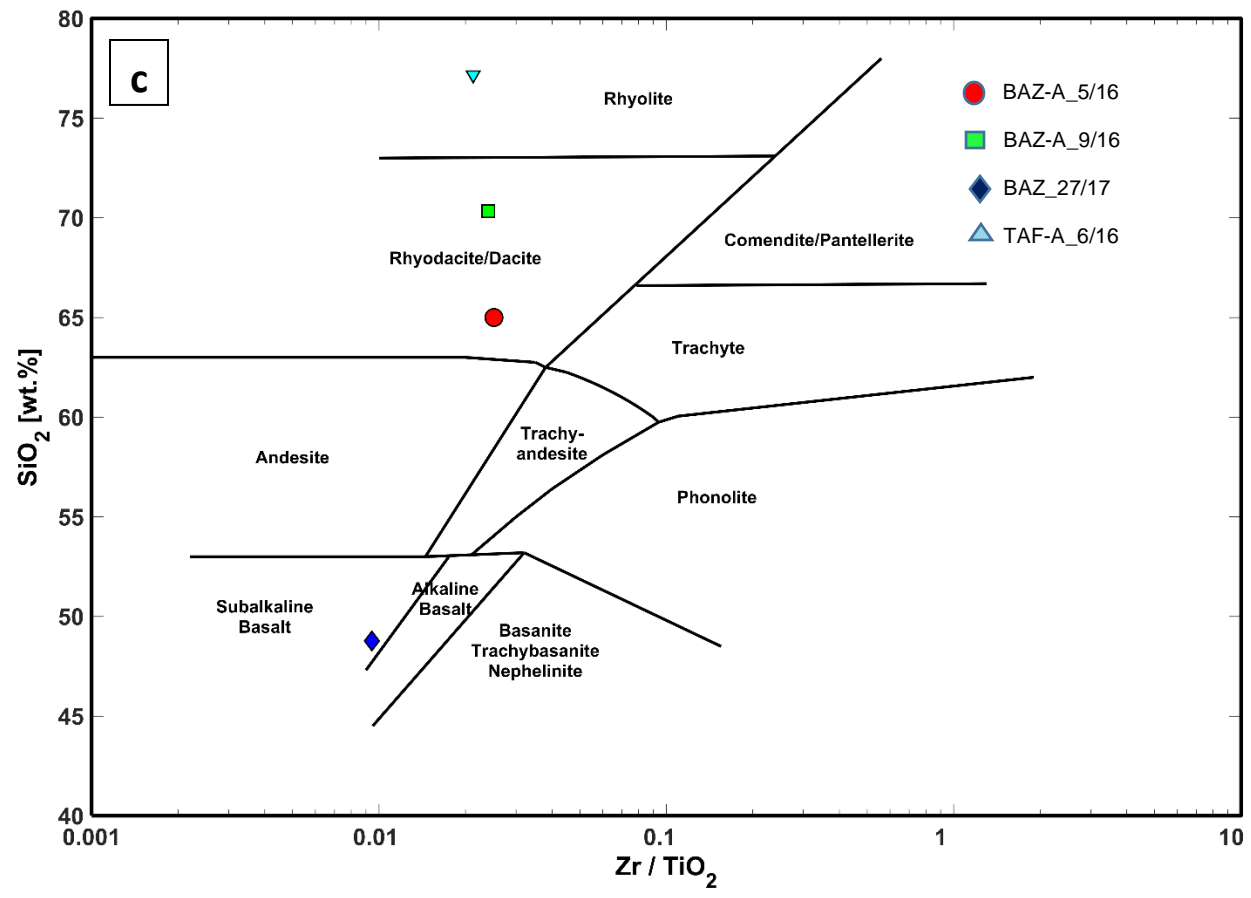
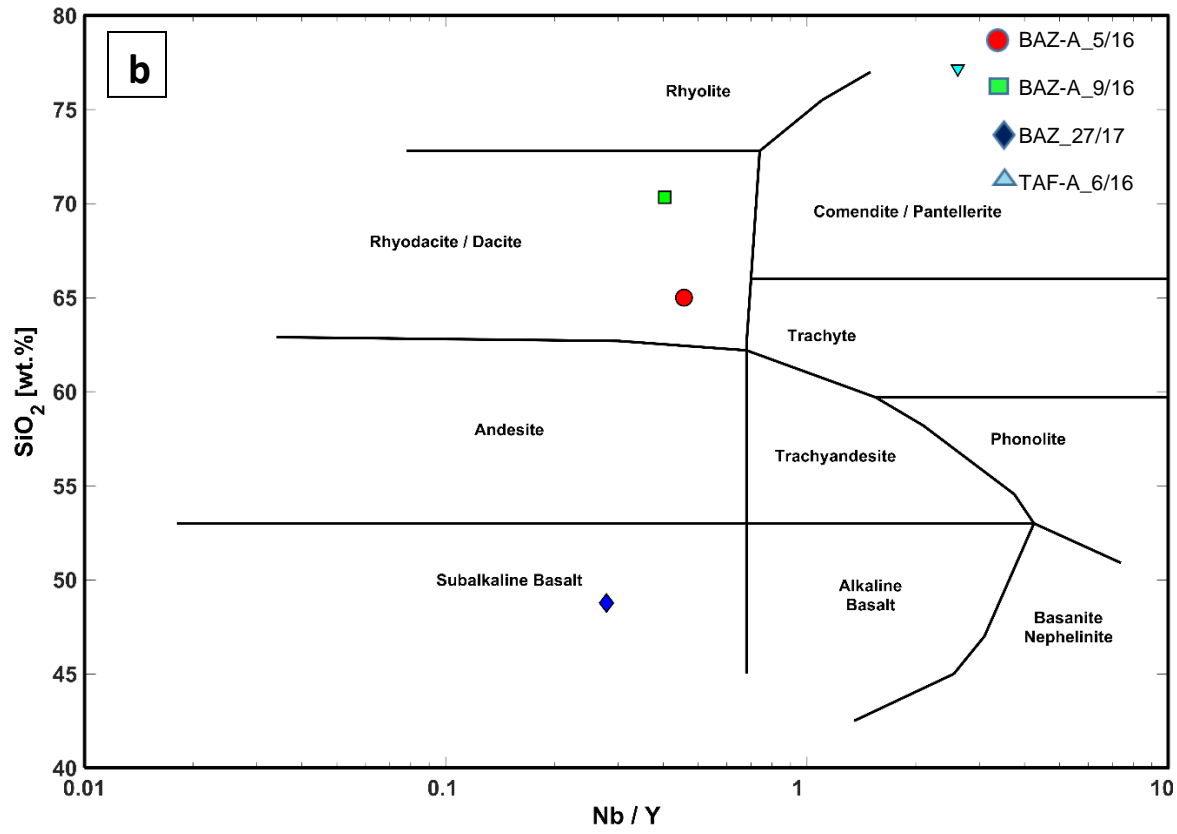


Fig. 3.10: Geochemical plots. (a) Total alkali-silica (TAS) diagram. Fields are from Le Bas et al. (1986). Analyses plotted have been recalculated 100% anhydrous (b) Nb/Zr vs SiO₂ (Winchester and Floyd 1977). (c) SiO₂ vs Zr/TiO₂ (Winchester flyod et al 1977)

These three plots show that the Bazman rocks are characterized into Alkaline Basalt and Dacite. The Taftan rock is characterized as Rhyolitic rock.

3.3 Earthquake Distribution of the study area

Using the real-time Earthquake data from IRIS and EHB, the below-shown image was generated using QGIS software.

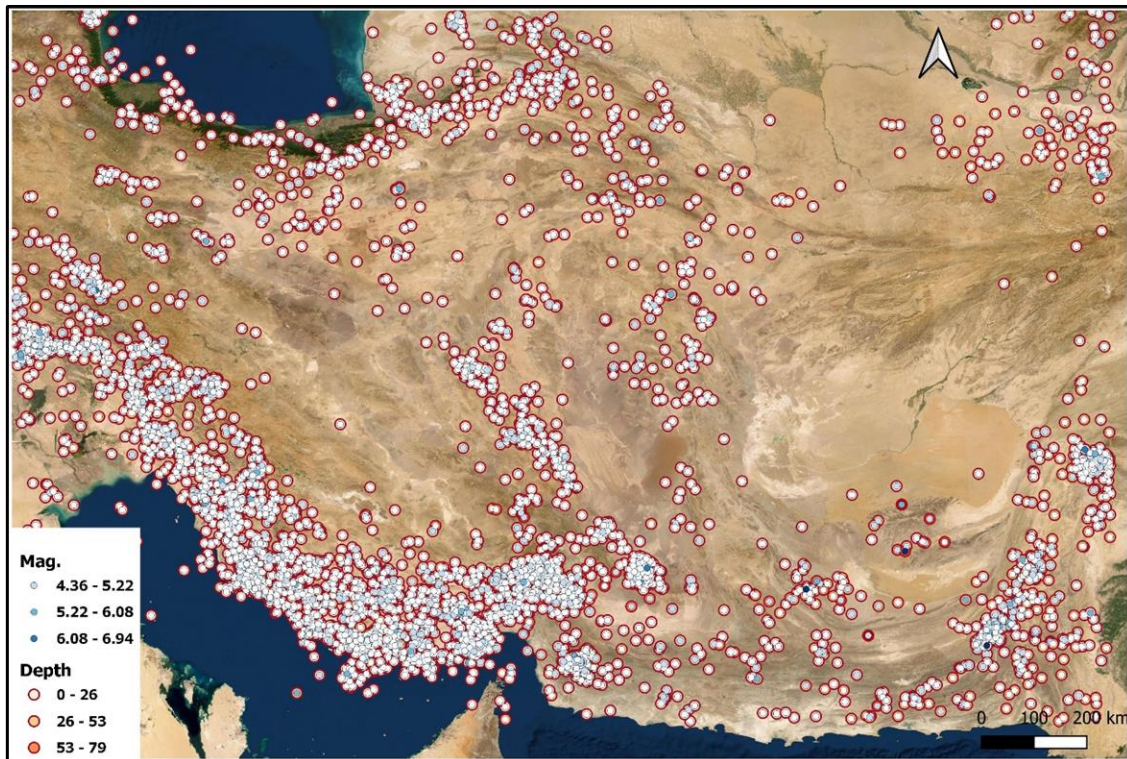


Fig. 3.11: The image shows the earthquake distribution with variation in magnitude and depth of earthquakes over the Iran region

3.4 Cross-section profiles of the study area (Depth vs Seismic velocity)

Below shows the results of cross-section profiles of the study area. Along four different transects cross-section profile was taken. The four different transects are-

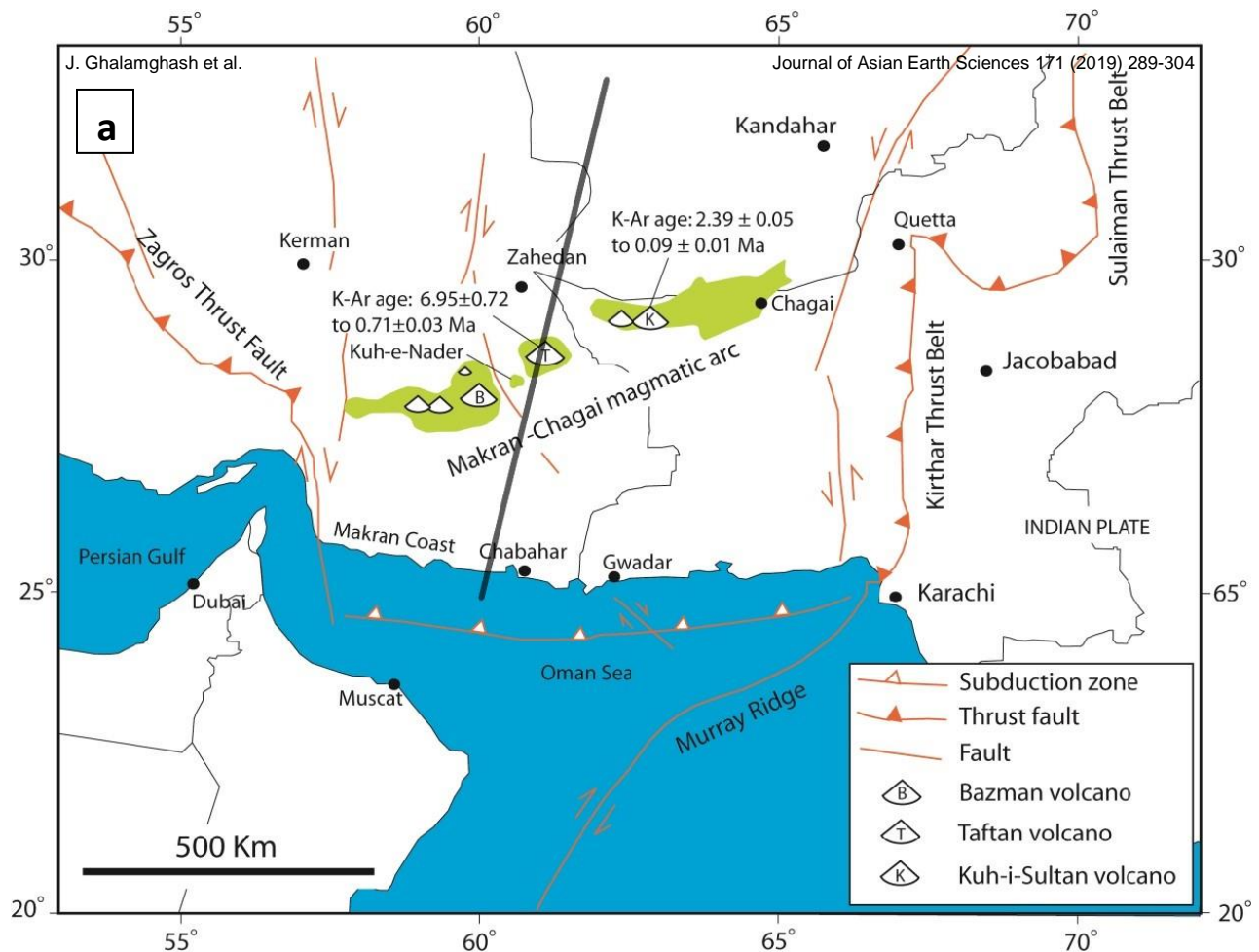
- a) 60E, 25N – 62E, 35N
- b) 63E, 25N – 65E, 35N

c) 64E, 25N – 61E, 35N

d) 60E, 28N – 67E, 30N

3.4.1 Transect along 60E, 25N – 62E, 35N

Transect for this profile is from 60E, 25N – 62E, 35N. This cross-section cuts across the Taftan volcanic region. The dark blue patches indicate a high-velocity region. Whereas the lighter blue indicates a slower velocity than the dark blue area. The dark blue high-velocity region is at a depth of approximately 80-140 km. The lighter blue patch is approximately 40 km.



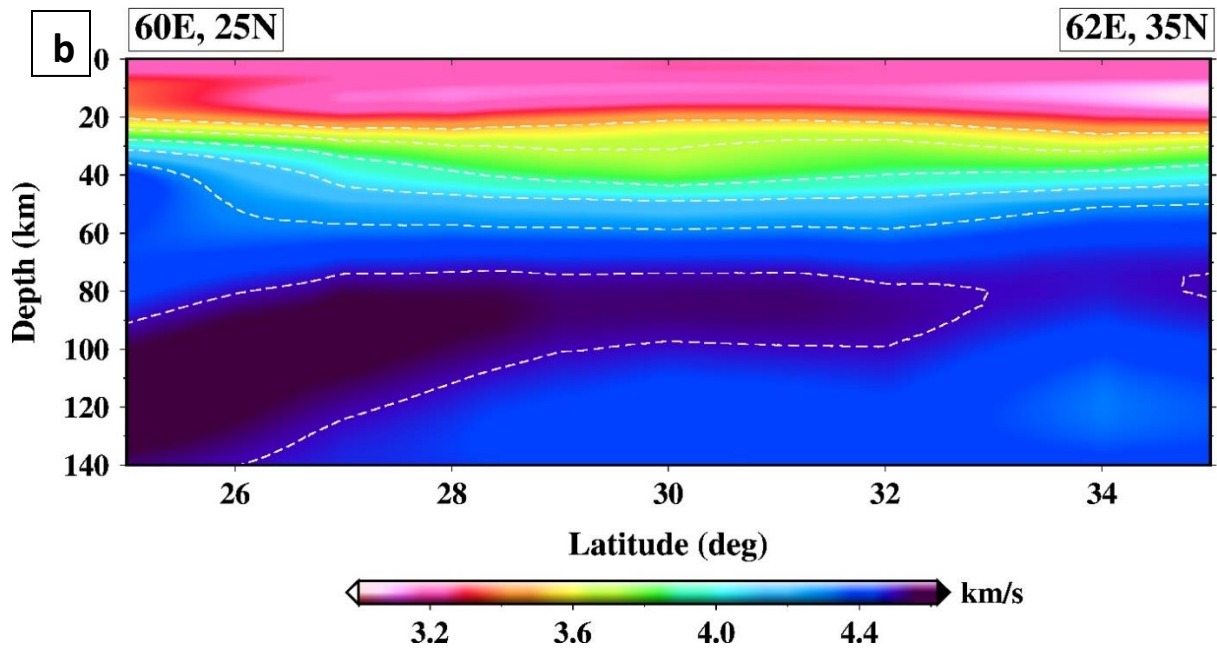
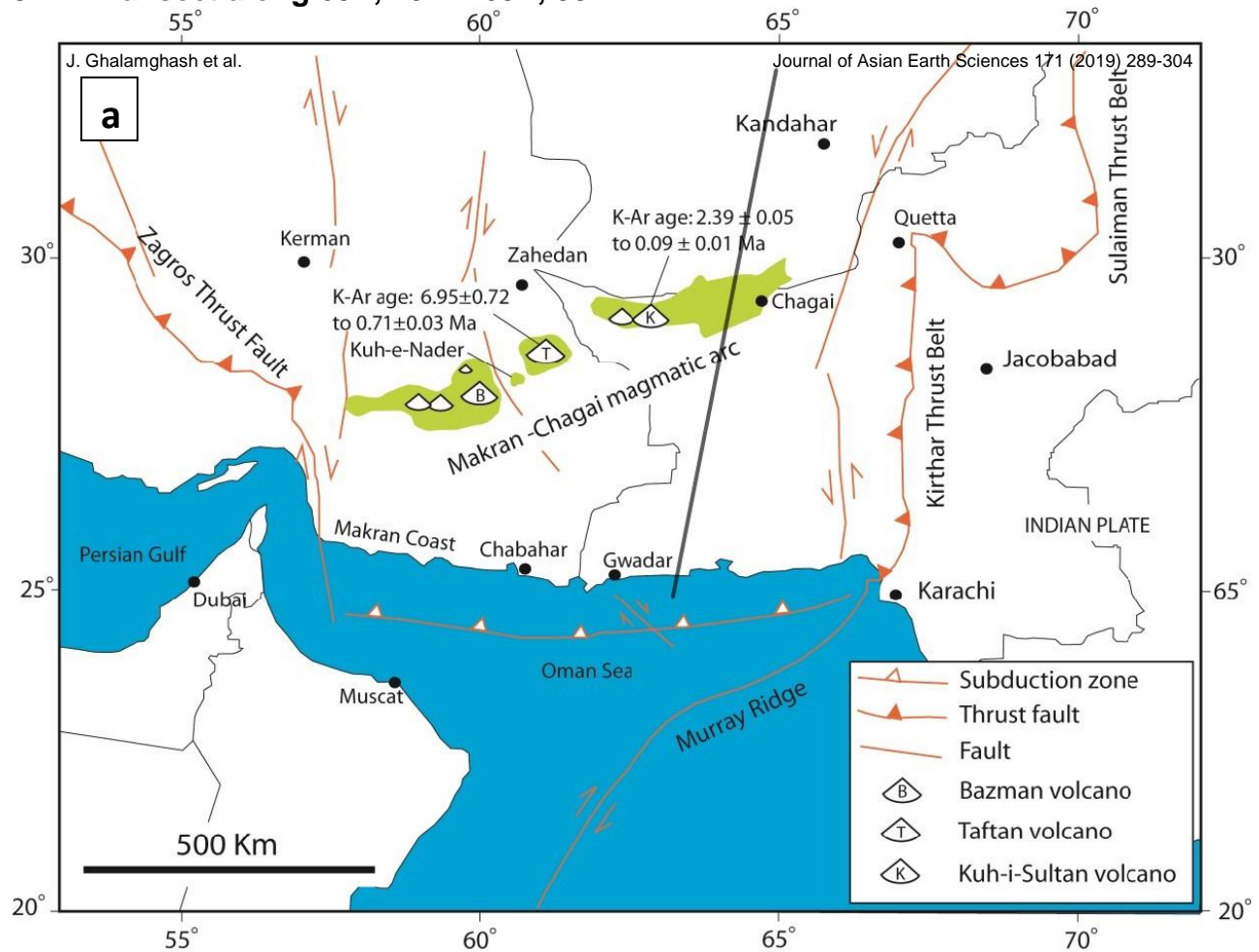


Fig. 3.12: (a) Image shows the cross-section profile on the Iran map. (b) Depth vs seismic velocity profile along the shown transect.

3.4.2 Transect along 63E, 25N – 65E, 35N



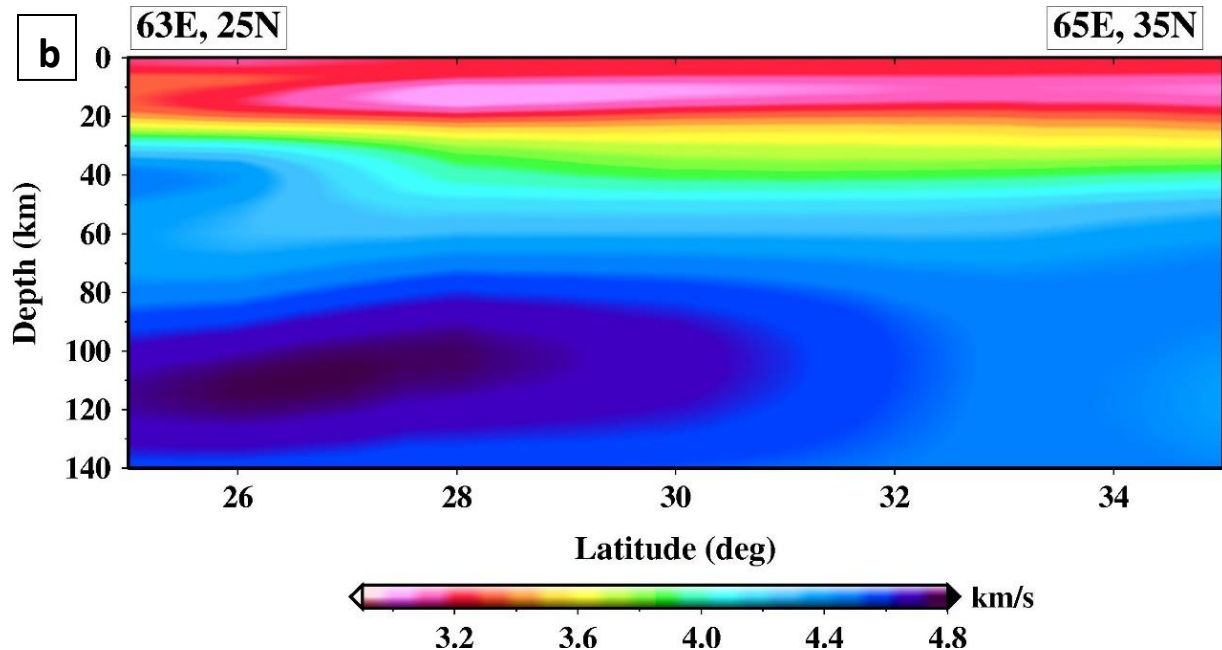


Fig. 3.13: (a) Image shows the cross-section profile on the Iran map. (b) Depth vs seismic velocity profile along the shown transect.

This cross-section profile is along the transect 63E, 25N – 65E, 35N, i.e. from the Oman sea and cutting across the Chagai magmatic arc. A big blob of high-speed velocity is observed around 100 km depth. The lower speed velocity zone is approximately around 40 km.

3.4.3 Transect along 64E, 25N – 61E, 35N

This transect passes through the Kuh-i-Sultan region, part of the Makran-Chagai volcanic arc. The profile is across the line joining these coordinates 64E, 25N – 61E, 35N. The high-speed velocity region is around 100 km. The low-velocity region at 40 km has reduced spatially in this profile.

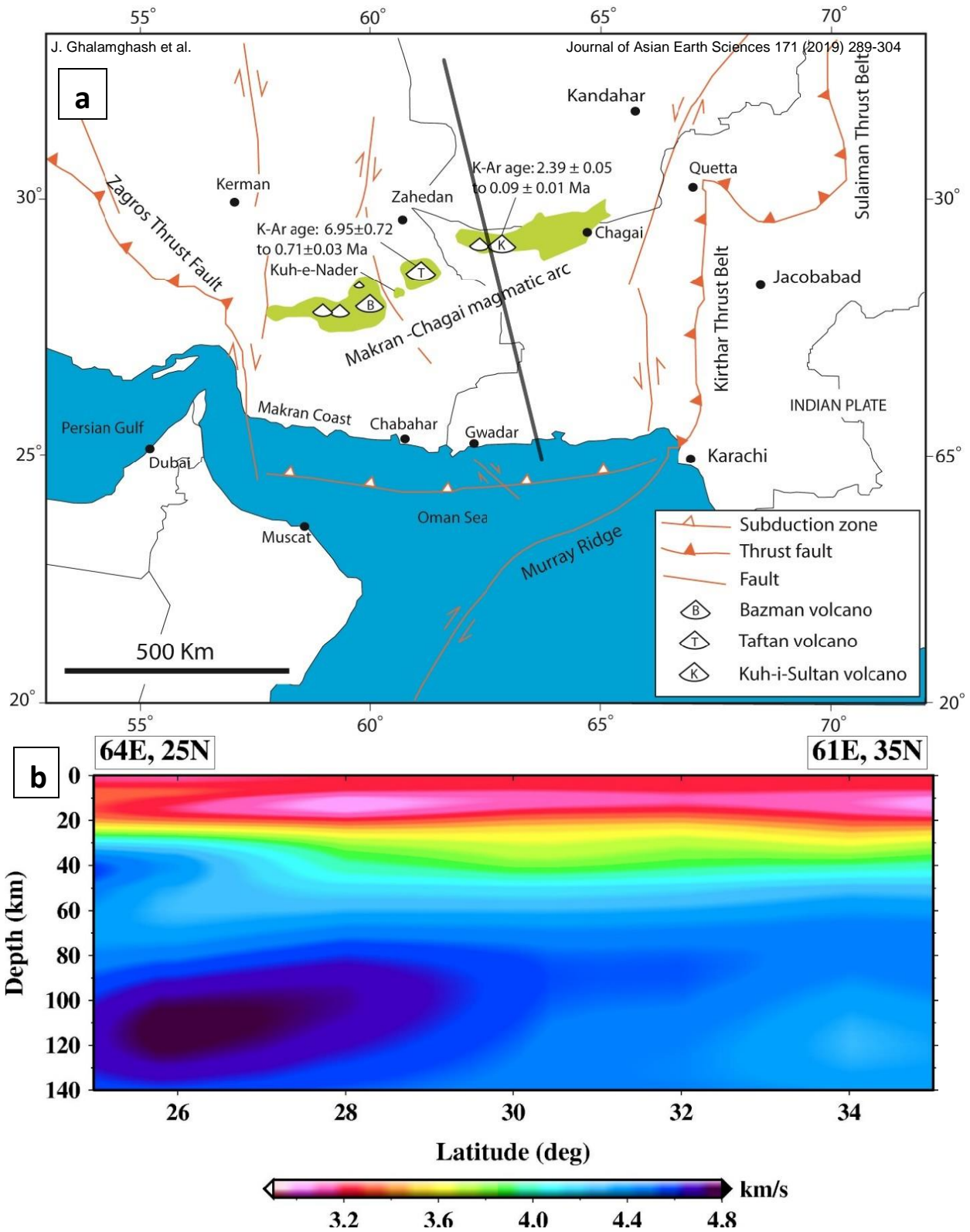
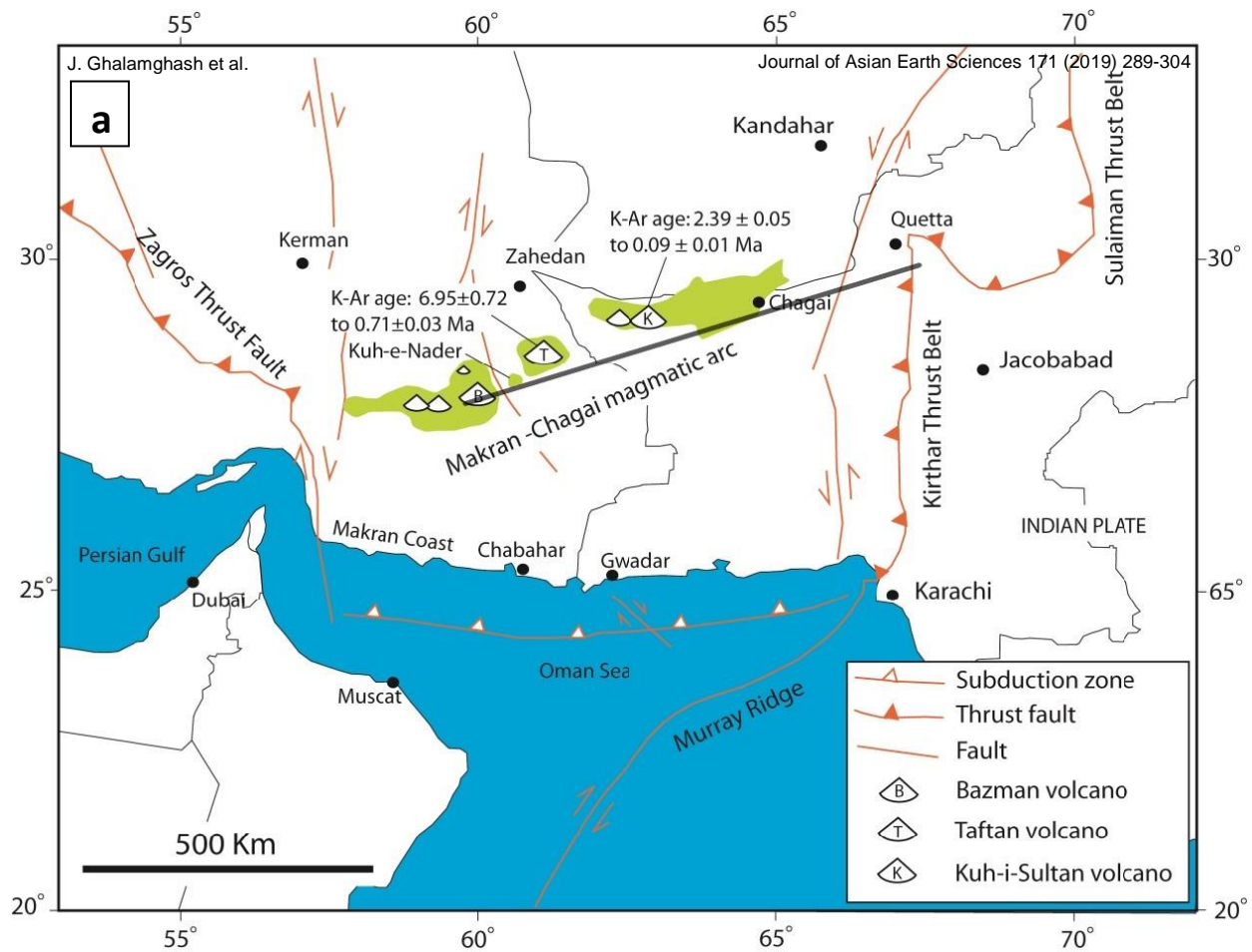


Fig. 3.14: (a) Image shows the cross-section profile on the Iran map. (b) Depth vs seismic velocity profile along the shown transect.

3.4.4 Transect along 60E, 28N – 67E, 30N

This profile is along the line joining the coordinates 60E, 28N – 67E, 30N. This cross-section profile tries to cover the profile across the complete Makran-Chagai magmatic arc. It passes through the Bazman volcanic region and goes straight till Quetta. The high-speed velocity profile is shifted towards the point 67E, 30N. The high velocity zone below the Kuh-e-Sultan stratovolcano is distinctly oval and occurs at a depth of 100 to 120 km bgl.



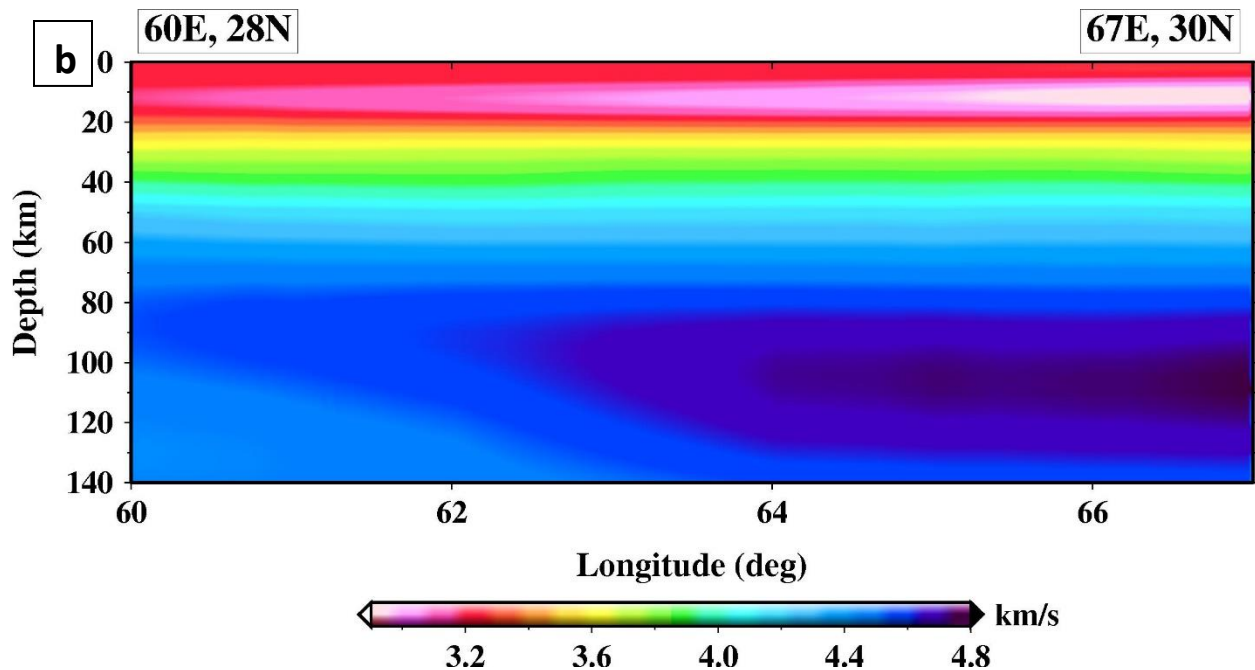


Fig. 3.15: (a) Image shows the cross-section profile on the Iran map. (b) Depth vs seismic velocity profile along the shown transect.

4. DISCUSSIONS

4.1 Petrography

Based on the petrographic observations, the samples are of lava flows which are highly vesicular. This indicates that the lava was highly reactive because of high volatile and gas content. The mesostatis of glass and plagioclase microlites with highly irregular vesicles imply that lavas have undergone huge strain amount. Many phenocrysts of Pyroxene also track down the high strain being acted while the eruption was occurring. The beautiful zoning shown by the Plagioclase euhedral phenocrysts is known as oscillatory zoning. This zoning implies that the Plagioclase crystal was growing when the magma chamber was forming.

4.2 Geochemistry

The whole rock oxide and trace element data helped in categorizing the type of rock based on its chemical composition. It can be said that according to the AFM diagram (write fig no.), the lava flows are not from the primary magma because they are depleted in the MgO content. The magma is evolved as the samples are lying closer to the Alkalis.

Because of fractional crystallization, the solid is removed hence the magma gets depleted in MgO and gets enriched in FeO.

The PI vs ASI plot is useful for the felsic rock classification. According to this, the rocks are falling under three categories which are peralkaline, metaaluminous and peraluminous. Two Bazman and one Taftan rock falls in metaaluminous region, i.e. the alkali content ($\text{CaO} + \text{Na}_2\text{O} + \text{K}_2\text{O}$) is more than the Aluminium oxide (Al_2O_3). Rest one Taftan and Bazman lies in peraluminous and peralkaline which means for peraluminous the Aluminium oxide is more than the alkali content and for peralkaline again the total alkali content but without CaO is more than the Aluminium Oxide.

From the plot of $\text{Na}_2\text{O} + \text{K}_2\text{O}$ vs SiO_2 , we characterize the rocks according to alkaline, sub alkaline and peralkaline. In this case, all three rocks, including Bazman and Taftan fall in sub alkaline region whereas one rock of Bazman is peralkaline in nature.

Na_2O vs K_2O plot shows that the Bazman rock samples belong to the Na-rich Magma series and the Taftan rock samples belong to the High K-rich magma series. From this plot, we characterized the rocks in two distinct types of igneous rocks.

From the SiO_2 vs Nb/Y plot, the Bazman rocks fall under the sub alkaline basalt, and Dacite category whereas the Taftan rock falls in Comendite igneous rock category.

In the SiO_2 vs Zr/TiO₂, the plot shows the same result as SiO_2 vs Nb/Y. The Bazman rocks are sub alkaline, and the Taftan rock is categorized as Rhyolite.

4.3 Cross-sectional Profiles (seismic velocity vs depth)

From all four cross-section profiles, it is visible that there are two high seismic velocity zones, i.e. one at ~40 km and the other at ~100 km. The 100 km dark blue region is of high seismic velocity zone. This zone is hot and plastic and therefore is related to partial melting. The northern edge of the high velocity zones in the seismic profiles matches well with the east-west axis of the Makaran-Chagi volcanic arc thereby validating the tectonomagmatic boundary of the extent of subduction of the oceanic lithosphere below the Oman Sea.

5. Conclusions

The study of the Taftan - Bazman volcanic area, South-eastern Iran and its relation with Makran-Chagai volcanic arc was done using Petrology, Geochemistry and Cross-section profiles.

- From all the analysis, the Taftan and Bazman volcanic area and the Makran-Chagai magmatic arc are related. The high velocity zones in the seismic profiles matches well with the east-west axis of the Makran-Chagai volcanic arc thereby validating the tectonomagmatic boundary of the extent of subduction of the oceanic lithosphere below the Oman Sea.
- From the cross-section profiles, the high seismic velocity zones show that there is a hot plastic slab beneath at 100 km depth and a probably a magma chamber at ~40 km depth.
- The Taftan and Bazman volcanic area is calc-alkaline type volcanism whereas the Bazo volcanic fields which represent small mono-genetic cinder cone volcanism are related to the Quaternary Shahsaravan volcanism of tholeiitic basaltic type.
- Based on Petrography, the rocks are volcanic in nature. The rocks are andesitic and Rhyolitic. Most of the rocks show high strain effects and the presence of volatiles and gases.
- The whole-rock major oxide and trace element analysis show that the rocks are calc-alkaline and tholeiitic. It shows that the tectonic setting was of convergent margin type.
- These conclusions also show that the stratovolcanoes are not extinct and can be at least of Vulcanian to sub-pilinian type. They are dormant and may erupt in future.

6. REFERENCES

1. Abdetedal M, Shomali ZH, Gheitanchi MR Crust and upper mantle structures of the Makran subduction zone in south-east Iran by seismic ambient noise tomography Solid Earth Discussions, (2014)
2. Arthurton R.S., Farah A. & Ahmed W., The Late Cretaceous-Cenozoic history of western Baluchistan Pakistan the northern margin of the Makran subduction complex

3. Biabangard H.& Moradian A. Geology and geochemical evaluation of Taftan Volcano, Sistan and Baluchestan Province, southeast of Iran Chinese Journal of Geochemistry volume 27, Article number: 356 (2008)
4. Conrad G., Montigny R., Thuizat R., Westphal M. Tertiary and quaternary geodynamics of southern Lut (Iran) as deduced from palaeomagnetic, isotopic and structural data (1981)
5. FastGAPP (Fast Geochemical Analysis Plotting Program) v2.0, A MATLAB based program, released 2012, The MathWorks, Inc., Natick, Massachusetts, United States.
6. Frost, B.R. and Frost, C.D. (2008) A Geochemical Classification for Feldspathic Igneous Rocks. *Journal of Petrology*, 49, 1955-1969. 10.1093
7. Ghalamghash, Jalil & Schmitt, A.K. & Shiaian, K. & Jamal, R. & Chung, Sun-Lin. Magma origins and geodynamic implications for the Makran-Chagai arc from geochronology and geochemistry of Bazman volcano, Southeastern Iran. *Journal of Asian Earth Sciences*. 171. 10.1016/j.jseaes.2018.12.006. (2018).
8. Lebas, M.J., Lemaitre, R.W., Streckeisen, A. and Zanettin, B. A Chemical Classification of Volcanic-Rocks Based on the Total Alkali Silica Diagram (TAS). *Journal of Petrology* 27(3): 745-750. (1986).
9. Michael M. Raith, Peter Raase & Jurgen Reinhardt Guide To Thin Section Microscopy Second Edition
10. Middlemost, E.A. Iron Oxidation Ratios, Norms and the Classification of Volcanic Rocks. *Chemical Geology*, 77, 19-26. (1989)
11. Mohammad Noor Sepahi Hazard Risk Assessment of the Taftan-Bazman Volcanic area, Baluchestan, Iran – a RS & GIS approach, PhD Thesis, August 2019
12. Petrology. Special sub-continent edition, 2nd edition, New York: Prentice Hall. Chapter 2- pg-53-56

13. Richards Jeremy P.; Wilkinson Damien; Ullrich Thomas Geology of the Sari Gunay Epithermal Gold Deposit, Northwest Iran* Economic Geology (2006) 101 (8): 1455–1496.
14. Seyed Amir Mohammad Razavi Khosroshahi (MS-Thesis), Geology, geochemistry, geochronology, and economic potential of the Taftan volcanic complex, south-eastern Iran 2015
15. Shand, S.J. Eruptive Rocks, Their Genesis, Composition Classification and Their Reaction to Ore-Deposits, with a Chapter on Meteorites. Murby, London. (1927)
16. Siebert L., and Simkin T., “Volcanoes of the world: an illustrated catalog of holocene volcanoes and their eruptions”. Smithsonian Institution. Global volcanism program digital information series, GVP-3. (2002).
17. Sourajit Sahoo, Petrography and geochemistry of the Kuh-e-Som pyroclastic cone, South-Eastern, Iran 2019
18. Verma SP, Torres-Alvarado IS, Sotelo-Rodríguez ZT (2002) SINCLAS: standard igneous norm and volcanic rock classification system. Comput Geosci 28:711–715
19. Winchester, J. & Floyd P. (1977). Geochemical discrimination of different magma series and their differentiation products using immobile elements. Chemical Geology. 20. 325-343. 10.1016/0009-2541(77)90057-2.
20. Winter, J. D. (2014). Principles of igneous and metamorphic
21. Zahra Firouzkouhi, Ali Ahmadi, David Richard Lentz and Ali-Asghar Moridi-Farimani Mixing of basaltic and andesitic magmas in the Bazman volcanic field of south-eastern Iran as inferred from plagioclase zoning. (2016)